

Review

# Historical and Current Landscapes of Autonomous Quadrotor Control: An Early-Career Researchers' Guide

Abner Asignacion, Jr.  and Suzuki Satoshi \* 

Graduate School of Engineering, Chiba University, Chiba 263-8522, Japan; abner\_asignacion@chiba-u.jp

\* Correspondence: suzuki-s@chiba-u.jp

**Abstract:** The rising demand for autonomous quadrotor flights across diverse applications has led to the introduction of novel control strategies, resulting in several comparative analyses and comprehensive reviews. However, existing reviews lack a comparative analysis of experimental results from published papers, resulting in verbosity. Additionally, publications featuring comparative studies often demonstrate biased comparisons by either selecting suboptimal methodologies or fine-tuning their own methods to gain an advantageous position. This review analyzes the experimental results of leading publications to identify current trends and gaps in quadrotor tracking control research. Furthermore, the analysis, accomplished through historical insights, data-driven analyses, and performance-based comparisons of published studies, distinguishes itself by objectively identifying leading controllers that have achieved outstanding performance and actual deployment across diverse applications. Crafted with the aim of assisting early-career researchers and students in gaining a comprehensive understanding, the review's ultimate goal is to empower them to make meaningful contributions toward advancing quadrotor control technology. Lastly, this study identifies three gaps in result presentation, impeding effective comparison and decelerating progress. Currently, advanced control methodologies empower quadrotors to achieve a remarkable flight precision of 1 cm and attain flight speeds of up to 30 m/s.

**Keywords:** quadrotors; autonomous flights; UAV control strategies; comparative survey; quadrotor tracking control review; quadrotor research trends; performance-based comparison; quadrotor history; early-career researchers



**Citation:** Asignacion, A., Jr.; Suzuki, S. Historical and Current Landscapes of Autonomous Quadrotor Control: Early-Career Researchers' Guide. *Drones* **2023**, *8*, 72. <https://doi.org/10.3390/drones8030072>

Academic Editor: Abdessattar Abdelkefi

Received: 16 January 2024  
Revised: 26 January 2024  
Accepted: 17 February 2024  
Published: 20 February 2024



**Copyright:** © 2023 by the authors. Licensee MDPI, Basel, Switzerland. This article is an open access article distributed under the terms and conditions of the Creative Commons Attribution (CC BY) license (<https://creativecommons.org/licenses/by/4.0/>).

## 1. Introduction

Quadrotors or quadcopters are unmanned aerial vehicles (UAVs) that possess four rotors. Their exceptional features have allowed for applications across diverse industries, indicating their potential as crucial assets in modern society. The distinctive characteristics include adaptability, mobility, and cost-effectiveness. The growing interest in quadrotors, as shown in Figure 1a, clearly demonstrates their appeal to both the public and researchers. Initially, these devices were mostly utilized by hobbyists and researchers. However, driven by the ease of availability of commercial products such as the Parrot AR.Drone and DJI drones, these devices have gained a wider attention. Furthermore, the proliferation of quadrotor applications such as aerial photography, search and rescue operations, industrial monitoring and maintenance, agriculture, entertainment, and potential future domains such as logistics and weather forecasting has contributed to their rising popularity.

Extensive research has been dedicated to quadrotor control [1,2], safe navigation [3], and their application across diverse fields [4]. As demonstrated in Figure 1b, the number of research papers focusing on quadrotor control has exhibited exponential growth, highlighting the significant attention directed toward advancing control methodologies for these aerial systems.

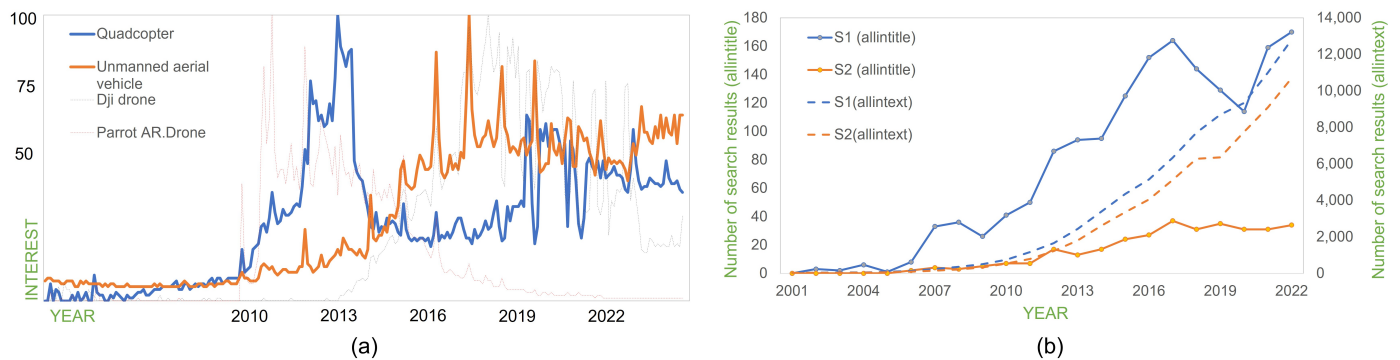


**Figure 1.** (a) A compelling evidence of the increasing interest among the general public in quadrotors or UAVs, as observed through Google Trends. The hype around quadcopter and UAV keywords can be attributed to the rising popularity of these two famous commercial drones: DJI drone and Parrot AR. Drone. (b) Proof of growing interest of researchers in quadrotor control, as evidenced by Google Scholar search results for two specific search prompts (S1 and S2) utilizing the *allintext* and *allintitle* criteria. S1: “(quadrotor OR quadcopter OR quad-rotor) AND (control)”, and S2: S1 “AND (trajectory OR tracking OR waypoint OR position)”. The emphasis is solely on the upward trend rather than the specific numerical values for each year, as the data may vary depending on Google’s algorithm.

### 1.1. Motivation

The primary objective for several research enthusiasts in the field of UAV applications is to realize quadrotor controllers aimed at applications such as autonomous flight, aerial manipulation, swarms, and multi-agent systems. Top controllers must exhibit exceptional performance in the face of disturbances, uncertainties, and faults. To suffice these necessities, researchers often turn to online libraries such as Google Scholar (GS) and IEEE Xplore (IX), where they anticipate finding high-quality controllers. Utilizing the search parameter “allintitle: S2” in GS may yield an impressive 67,500 results, while conducting an abstract-based search in IX Advanced Search produces 1205 results. By narrowing the scope to the past decade, the GS presented 22,000 relevant findings compared to the IX’s 1082. Further limiting the search to the last five years, it was observed that GS resulted in 18,700 matches while IX yielded 629 matches. The first notable papers in the list of GS include [5–9], whereas those in IX are [10–14]. These papers propose an array of control strategies encompassing learning (Lrn) [5,10,11], sliding mode control (SMC) [14], optimal techniques (Opt) [8], disturbance estimation [9], backstepping (Bk) [10,12], and hybrid controllers [6,7,13]. Although the number of search results may vary depending on the time of the search, the amount of published information to digest remains overwhelming for researchers within a limited time. For instance, when early-career researchers in this field are confronted with challenging choices, they are often unsure of the best path to follow. A few of the key questions that emerge include:

- Are these controllers truly cutting-edge?
- Where should their focus be directed?
- How can they fine-tune the control parameters?

Despite these doubts, every paper appears to be promising. This dilemma is unique to early-career researchers, especially those who are encouraged to independently learn quadrotor control and those who do not learn around experts. Motivated by the aforementioned dilemma, the researchers sought reviews to guide their decisions. In addition, gathering insights from other researchers regarding their selected methods may provide valuable clarity.

Several review papers have extensively covered various aspects of UAVs, including the classification, modeling/identification, control, planning, sensing/estimation, and applications. These comprehensive reviews serve as valuable learning platforms to students

and practitioners. Figure 2 shows a collection of 16 review papers [2,15–29] on UAV control published a decade ago, featuring components, citation counts, and reference quantities.

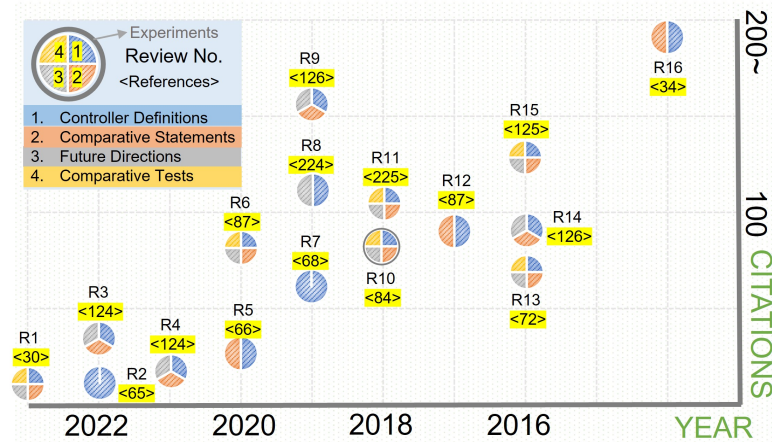


**Figure 2.** Existing review articles on quadrotor control, highlighting number of references and citations as indications of article comprehensiveness and impact. While these alone do not determine the quality of review, they reflect the breadth of research considered in the article, along with potential helpfulness to the readers. Review numbers are as follows: [15] (R1), [16] (R2), [17] (R3), [18] (R4), [19] (R5), [20] (R6), [21] (R7), [22] (R8), [23] (R9), [24] (R10), [25] (R11), [26] (R12), [27] (R13), [28] (R14), [2] (R15), [29] (R16).

The survey in [22] focused on the position and attitude control of UAVs, highlighting the prevalence of cascade control and demonstrating the feasibility of robust tracking control in quadrotors. However, it fails to provide systematic or in-depth analysis and does not synthesize current studies to identify existing gaps. Ref. [15] compared several attitude control methods in hierarchical structure, where the tracking control is only a PID control. Ref. [20] compared four path-following controls.

To establish a comprehensive review, ref. [25] discussed modeling, system identification, control algorithms, and obstacle avoidance. Detailed comparisons of the controllers (PID, feedback linearization (FL), SMC, and integral Bk) through numerical simulations reveal SMC's superior tracking precision and robustness, whereas PID excels in energy efficiency. In contrast, ref. [2] compared five controllers (PID, FL, SMC, Bk, and fuzzy control) using nine performance metrics. The authors performed a two-step parameter-tuning strategy wherein the attitude control must first obtain a satisfactory response, and the position control parameters are then tuned. The findings of this study designate SMC and Bk as highly accurate yet computationally demanding control strategies. Conversely, while exhibiting less demanding computational requirements, the FL controller yielded relatively inferior results. The PID controller is the simplest model, and it exhibits the smallest tracking error under nominal conditions. However, it is susceptible to disturbances. The authors posited that SMC strikes a good balance between the control performance and inherent simplicity, thereby advocating its efficacy in practical applications.

In [25], a tutorial-like exposition-covered SMC, model reference adaptive control (MRAC), and adaptive SMC were proposed for quadrotor autopilots. Detailed experiments assessed the implementability, tracking performance, and computational load, ultimately favoring adaptive SMC. However, the review does not provide sufficient evidence to support the initial choice of SMC based on popularity and plans to expand its scope in future work.

Considering [15], SMC takes the spotlight as the most robust and most balanced controller after using several statistical analysis methods. However, different trends were observed when practitioners and young researchers were asked about their preferences. They learned to use PD and optimal control methods instead of SMC. This discrepancy raises questions regarding the true state-of-the-art controllers in the UAV field. Furthermore,

complex aspects such as coupling, control structure, and verification methods contribute to the complexity. Therefore, a more thorough approach is required to bridge these gaps.

### 1.2. Contribution

The main challenge in existing review papers is the limitation of covering broad topics, which makes it difficult to conduct in-depth analyses. In this study, we address this issue by primarily focusing on quadrotor trajectory-tracking control (QTTC) and its coupling with attitude control, as illustrated in Figure 3. This area is highly significant within the high-level control framework of autonomous quadrotor flight, which involves precise trajectory execution and tracking in demanding environments. Autonomous quadrotor flight involves self-directed navigation and maneuvers, excluding human intervention. Relying solely on attitude control proves inadequate; a well-designed QTTC is imperative. Furthermore, QTTC offers solutions to handle disturbances and uncertainties, which are critical aspects of quadrotor applications such as aerial photography, search and rescue missions, inspections, and goods delivery. Recent advancements in sensors, processors, and algorithms have resulted in the ease of implementation of autonomous flights. This has further enabled drones to navigate complex environments autonomously and reduced human intervention and associated risks. Swarms and fleets of autonomous drones can work together to provide greater scalability and coordination. Moreover, Pixhawk, a popular open-source autopilot system utilized in UAVs, incorporates built-in stabilizing attitude control capabilities. Therefore, the design of the tracking control is significantly for integration in autonomous flight. Despite its importance, to the best of the authors' knowledge, there have been no comprehensive review papers on this topic to date. We considered more than 300 published works, although not all were included in the references due to the length limit of the paper.

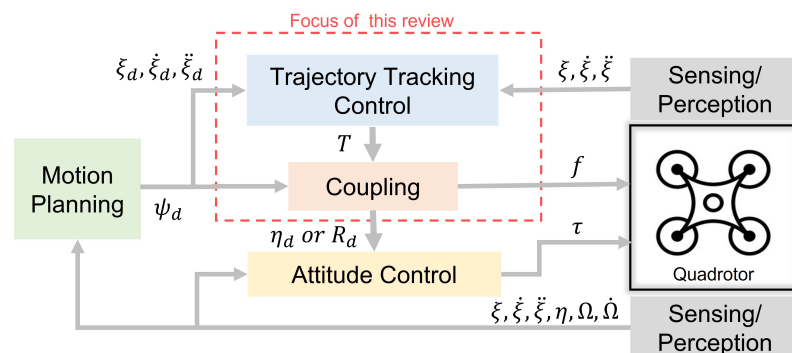


**Figure 3.** Autonomous quadrotor control system structure spotlighting our research focus.

The main contributions of this study are as follows:

1. In Section 2, we present a brief historical overview that has significantly influenced the current control technologies applied to quadrotors.
2. In Section 3, we provide a comprehensive data-based review of peer-reviewed literature on QTTC over the past decade. This review covers various aspects, including modeling, verification, control structures, control input terms, and techniques used to address under-actuation.
3. In Section 4, we identify five major trends from the past decade to facilitate an improved analysis and grouping of papers based on their control objectives. Furthermore, we incorporate several tables to clearly illustrate the disparities in the performances among high-impact publications. This process highlights bottlenecks that impede progress in this field through data-based analysis and proposes solutions to address these challenges.
4. In Section 5, we unveil the state-of-the-art control methods based on our comprehensive analysis. Additionally, we offer insights into the challenges associated with selecting an appropriate controller for a specific application and provide suggestions to overcome these hurdles.

These contributions aim to foster a comprehensive understanding of QTTC and offer guidance to early-career researchers and practitioners in the field. Table 1 presents the nomenclature employed to facilitate discussions.

**Table 1.** Nomenclature: system variables and inputs.

Variable	Meaning	Variable	Meaning
$\xi$	position	$f$	input force
$v$	velocity	$\tau$	input torque
$a$	acceleration	$d$	disturbance force
$\eta$	attitude angles	$e_\xi$	position error
$\Omega$	angular rate	$\diamond_d$	desired value of $\diamond$
$\omega$	motor angular speed	$\widehat{\diamond}$	estimated $\diamond$
$m$	mass	$K_p$	P gain
$K_f$	aerodynamic param	$K_d$	D gain
$I$	moment of inertia	$k$	design parameters
$I_r$	motor's $I$	$\chi$	observer/Bk variables
$g$	gravitational acc	$\beta$	method-dependent variables

## 2. A Brief Historical Overview of QTTC (Beginning to 2013)

The history of quadrotor technology includes a combination of advancements in various fields, including aerodynamics, control theory, computer science, and robotics. Figure 4 illustrates the evolution of quadrotor technology as a tree growing from its first seed to the catalysts that have driven its development, culminating in the impressive capabilities of modern quadrotors.

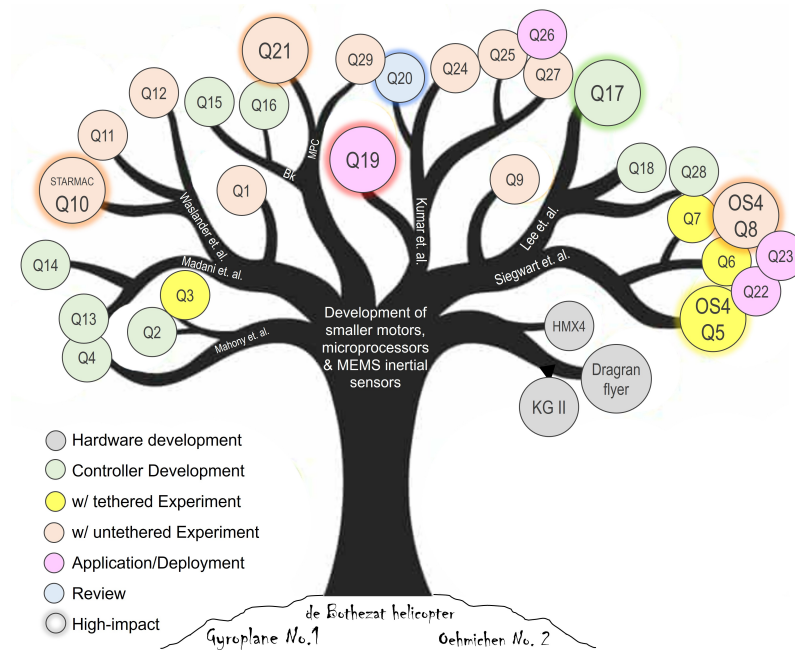


**Figure 4.** Quadrotor technology evolution: a tree of progression with roots in first-generation quadrotors, catalyst-driven branches of advancement, and fruits of inspirational achievements from leading laboratories. Quadrotor research reference numbers are as follows: [30] Q1, [31] Q2, [32] Q3, [33] Q4, [34] Q5, [35] Q6, [36] Q7, [37] Q8, [38] Q9, [39] Q10, [40] Q11, [41] Q12, [42] Q13, [43] Q14, [44] Q15, [45] Q16, [46] Q17, [47] Q18, [48] Q19, [49] Q20, [50] Q21, [51] Q22, [52] Q23, [53] Q24, [54] Q25, [55] Q26, [56] Q27, [57] Q28, [58] Q29.

The quadrotor concept traces its roots back to 1907 with the development of Gyroplane No.1, a large-scale aircraft that spans 8 m and weighs 578 kg. However, small-scale quadrotors only emerged nearly a century ago. A notable breakthrough occurred in 1989 with

the introduction of Keyence GyroSaucer II E-570 (Japan), marking a significant milestone in quadrotor development. Subsequently, successful models, such as the Draganflyer and Roswell flyer (HMX-4), emerged in 1999, heralding the era of hobbyist kits. These advancements have been made possible by the progress in microprocessor capabilities and the availability of microelectromechanical (MEMS) inertial sensors [30].

At the ROMAN 2001 workshop, a feedback controller based on a linearized dynamic model was presented. Simulation studies have been conducted to evaluate its performance [31]. In 2002, a collaboration between the GRASP Lab of UPenn and R. Mahony of the Australian National University involved the testing of a camera-equipped HMX-4 quadrotor [32]. However, the performance was affected by the tethering system. Consequently, a dynamic-model-based Bk control ( $\tau_i \rightarrow (\xi, \psi_d)$ ) was developed to stabilize the quadrotor during quasi-stationary flight conditions [33]. The dynamic model is described by Newton's equations.

$$\begin{aligned}
 \dot{\xi} &= v \\
 \dot{v} &= ge_3 - \frac{1}{m}fRe_3 \\
 \dot{R} &= Rsk(\Omega) \\
 I\dot{\Omega} &= -\Omega \times I\Omega + G_a + \tau \\
 I_r\dot{\omega}_i &= \tau_i - Q_i \\
 R &= \begin{bmatrix} c_\theta c_\psi & s_\theta c_\psi & c_\phi c_\theta c_\psi + s_\phi s_\psi \\ c_\theta s_\psi & s_\theta s_\psi & c_\phi s_\theta s_\psi - s_\phi c_\psi \\ -s_\theta & s_\phi c_\theta & c_\phi c_\theta \end{bmatrix}
 \end{aligned} \tag{1}$$

where  $R$  is the rotation matrix,  $I_r$  is the moment of inertia of each motor,  $\tau_i$  is the torque exerted of each motor,  $e_3$  is  $[0 \ 0 \ 1]^\top$ , and  $sk(\Omega)v = \Omega \times v$  is the skew-symmetric matrix. The motor dynamics account for aerodynamic drag as  $Q_i = \kappa\omega_i^2$ , where  $\kappa$  is a constant. The desired force vector from Bk is obtained as

$$\begin{aligned}
 T &= mge_3 + m\ddot{\xi}_d - mk_1(k_1 + k_2)\beta_1 \\
 \beta_1 &= \frac{1}{k_1}(v - \dot{\xi}_d) + (\xi - \xi_d)
 \end{aligned} \tag{2}$$

where  $\ddot{\xi}_d$  denotes desired acceleration. The reference for attitude control is the desired rotation matrix, as shown below:

$$R_d e_3 = \frac{T}{\|T\|} \tag{3}$$

where  $\|T\|$  denotes the 2-norm of  $T$ . A stabilization experiment for take-off, hovering, and landing was conducted by Castilio et al. using Lagrange dynamic modeling and a controller based on nested saturation.

$$\begin{aligned}
 m\ddot{\xi} &= mge_3 - fRe_3 \\
 I\ddot{\eta} &= -C(\eta, \dot{\eta})\dot{\eta} + \tau
 \end{aligned} \tag{4}$$

where  $-C(\eta, \dot{\eta})\dot{\eta}$  is the Coriolis term that contains the gyroscopic and centrifugal terms.

In 2004, Autonomous Systems Lab (ASL), led by R. Siegwart, launched the OS4 Project with the aim of enabling the fully autonomous navigation of micro vertical take-off and landing (VTOL) vehicles, including quadrotors, within indoor environments [34]. In the same year, attitude controllers ( $\tau \rightarrow \eta$ ) were developed using the PID and LQR control strategies, and their attributes were compared in detail [35]. In 2005, two nonlinear QTTC methods were designed and evaluated using the OS4 test bench. These methods aimed to obtain  $T$  and  $\tau$  to accurately track the desired trajectories  $(\xi, \psi_d)$  using the Bk and SMC techniques [36]. By 2007, the OS4 quadrotor, weighing 520 g and equipped with BLDC (brushless DC) motors, a 40 g on-board computer module, a camera, and a 230 g lithium

polymer battery, was constructed [37]. It achieved untethered flight, and a hierarchical integral Bk QTTC  $((T, \tau) \rightarrow (\zeta, \psi_d))$  structure was employed for testing and evaluation.

$$f = \frac{mg - \beta_1}{\cos \phi \cos \theta} \tag{5}$$

where  $\beta_1 = (1 - k_1^2 + k_2)e_z + (k_1 + k_3)\beta_2 - k_1k_2 \int_0^t e_z d\tau_t$ , and  $\beta_2 = k_1e_z + \dot{e}_z + k_2 \int_0^t e_z d\tau_t$ .  $e_z$  is the error variable of the  $z$  position. It should be noted that the force control input is solely dependent on the altitude. Under the small-angle assumption, the desired roll and pitch angles were obtained, as shown below:

$$\begin{bmatrix} \phi_d \\ \theta_d \end{bmatrix} = \begin{bmatrix} -u_y \\ u_x \end{bmatrix} \tag{6}$$

where  $u_x$  and  $u_y$  are the horizontal axis inputs obtained using the chosen position controller. The attitude and position loops were operated at frequencies of 76 and 25 Hz, respectively, to prevent spectral conflicts caused by time-scale separation. It successfully tracked a 2 m square trajectory with a 20 cm overshoot in 20 s. This work was complemented by [38] by not making a small-angle assumption to be achieved.

$$\begin{bmatrix} \phi_d \\ \theta_d \end{bmatrix} = \begin{bmatrix} \arcsin \frac{m(u_x s_{\psi_d} - u_y c_{\psi_d})}{f} \\ \arcsin \frac{m(u_x c_{\psi_d} + u_y s_{\psi_d})}{f c_{\phi_d}} \end{bmatrix} \tag{7}$$

In the same year, Stanford University introduced STARMAC II, weighing less than 2.5 kg and equipped with an attitude PID control system that accounts for three quantifiable aerodynamic effects that can be compensated for by attitude control [30]. In 2008, a PID QTTC was designed for STARMAC II, which enabled a 0.8 m square trajectory with errors of 10 cm indoors and 50 cm outdoors, surpassing the commercial global navigation satellite system (GNSS) drone MD4-200 by achieving a 2 m accuracy outdoors with a velocity of 0.5 m/s [39]. In the following year, the STARMAC team attempted to overcome the aerodynamic effects on aggressive flights (approximately 8 m/s) [40] and wind disturbances [41], resulting in a more agile and robust controller.

The full-Bk QTTC  $(\omega_i \rightarrow (\zeta, \psi_d))$  was proposed by Madani et al. in [42] and divided the quadrotor system into three subsystems: (S1)  $x, y, \phi$ , and  $\theta$ ; (S2) altitude and yaw angle; and (3) motor speed [43]. The aerodynamic effects are considered to be the additive force and torque rather than motor dynamics.

$$F_{aero} = K_f v \tag{8}$$

Their fixed experimental setup could only verify the altitude and yaw angle tracking performance, which were affected by poor sensor measurements. They also presented a Bk-SMC that integrated the SMC in [42] into a three-subsystem full-Bk control technique. Theoretically, a robust Bk QTTC was developed in accordance with parametric uncertainties with a global uniform ultimately bounded (GUUB) tracking error guarantee via Lyapunov stability analysis; however, no simulation or experiment was performed. In 2010 [44], command-filtered compensation was proposed to address the problem of the Bk control of analytical derivative expressions. This result is similar to the nonlinear coupling proposed by [45] in 2009. The force control input and the desired attitude are obtained as follows:

$$f = m(u_x R_{13} + u_y R_{23} + u_z R_{33}) \tag{9}$$

$$\begin{bmatrix} \phi_d \\ \theta_d \end{bmatrix} = \begin{bmatrix} \arcsin \left( \frac{m(u_x s_{\psi_d} - u_y c_{\psi_d})}{u_T} \right) \\ \arctan \left( \frac{(u_x c_{\psi_d} + u_y s_{\psi_d})}{(u_z + g)} \right) \end{bmatrix} \tag{10}$$

where  $R_{13} = c_\phi c_\theta c_\psi + s_\phi s_\psi$ ,  $R_{23} = c_\phi s_\theta s_\psi - s_\phi c_\psi$ ,  $R_{33} = c_\phi c_\theta$ , and

$$u_T = m \sqrt{u_x^2 + u_y^2 + (u_z + g)^2} \quad (11)$$

where  $u_x$ ,  $u_y$ , and  $u_z$  are designed using PID control for each position state, and  $s_\diamond$  and  $c_\diamond$  are the sine and cosine of the  $\diamond$  angle, respectively. This effectively separates the translational and rotational dynamics and solves the timescale separation problem.

In [46], a revolutionary idea proposed a geometric approach and introduced geometric tracking control wherein the force control input was used to obtain the desired rotation matrix, as shown below:

$$\begin{aligned} R_d e_3 &= R_{d3} = \frac{T}{\|T\|} \\ R_{d2} &= R_{d3} \times [c_{\psi_d} \quad s_{\psi_d} \quad 0]^\top \\ R_{d1} &= R_{d2} \times R_{d3} \end{aligned} \quad (12)$$

Obtaining  $R_{d3}$  is similar to obtaining (3) from 2004 onward. The assumption  $\|T\| \neq 0$  is reasonable from both theoretical and practical standpoints. When  $\|T\| \neq 0$ , the quadrotor is in free-fall motion or the propellers stop, and this should be avoided at all costs in practical applications. Then, the force control input and desired attitude can be expressed as

$$T = m g e_3 + m \ddot{\zeta}_d - K_p e_\zeta - K_d \dot{e}_\zeta \quad (13)$$

$$f = (R_{d3})^\top T \quad (14)$$

$$R_d = [R_{d1} \quad R_{d2} \quad R_{d3}] \quad (15)$$

where  $e_\zeta = \zeta - \zeta_d$  and  $\dot{e}_\zeta = v - \dot{\zeta}_d$ . This is similar to the simplified (2). At low accelerations, the feedforward terms can be ignored; however, at higher accelerations, the controller performance can be significantly improved. A robust approach to bounded uncertainties was proposed by these authors [47].

At ICRA 2011, the most cited paper on quadrotor control was written by Kumar. Their paper demonstrates the combination of the controller design and trajectory generation for quadrotor maneuvering in constrained indoor environments [48]. The proposed technique utilizes the differential properties of quadrotors and expresses the control input as an algebraic function of four carefully selected flat outputs and their derivatives. This ensures the generation of smooth trajectories (minimum snaps) that the quadrotor can follow. This approach adopts a geometric method aimed at obtaining the desired attitude from Equation (15) and the force control input from Equation (14). Experimental results obtained using the Vicon motion capture system demonstrated a position error of less than 8 cm for an Ascending Technologies Hummingbird quadrotor (500 g) flying through thrown circular hoops. The quadrotor followed a highly aggressive trajectory with a velocity of up to 3.6 m/s. He also presented in TEDtalks, showing the capabilities and applications of UAVs as early as 2012 ([https://www.youtube.com/watch?v=4ErEBkj\\_3PY](https://www.youtube.com/watch?v=4ErEBkj_3PY)) (last accessed on 16 February 2024). The C code utilized for Bitcraze's Crazyflie is accessible online ([https://github.com/bitcraze/crazyflie-firmware/blob/master/src/modules/src/controller/controller\\_mellinger.c](https://github.com/bitcraze/crazyflie-firmware/blob/master/src/modules/src/controller/controller_mellinger.c)) (last accessed on 16 February 2024).

R. Mahony, V. Kumar, and P. Corke collaboratively wrote a tutorial paper [49] that addressed the modeling, estimation, and control of quadrotors. This study highlights three main challenges in QTTC: underactuation, aerodynamic effects, and force/torque-to-motor-speed conversion.

In 2012, ref. [50] implemented a model predictive control (MPC) for QTTC in accordance with system constraints and atmospheric disturbances. The dynamic model was transformed into piecewise affine models around the nominal operating points. The MPC was designed based on three subsystems—attitude, horizontal, and altitude—considering the state, input, and rate of change in the control input. The underactuation was addressed according to the approach in [44]. This pioneering work demonstrated the implementation

of MPC in a real trajectory-tracking flight with an attitude control loop running at 120 Hz and a position control loop running at 33 Hz. The results show a deviation of 2.64 cm on the y-axis and 0.5 cm on the z-axis when following a line trajectory, even in the presence of wind gusts. The prediction horizon was set to five, and the control horizon was set to two for all subsystems. The experiment utilized a 1.1 kg UPATcopter equipped with a Kontron™ pITX single-board computer, and position data were obtained by fusing IMU, sonar, and optical flow sensor data using an extended Kalman filter (EKF).

Several researchers have proposed SMC-based quadrotor control. Ref. [59] divides the system into two, similar to [42] but without the S3, and designs an SMC control for each subsystem. The adaptive SMC is designed using a feedback-linearized model [60]. In [61], a simple trajectory-tracking experiment was performed on an AR drone to compare high-order terminal SMC, SMC, and PID controls. High-order SMC (HOSMC) is a technique that avoids the chattering phenomenon by using a continuous signal, whereas terminal SMC (TSMC) promotes fast tracking. The results demonstrated values of 8.96, 15.62, and 13.14 cm, respectively, demonstrating the superiority of TSMC over PID control.

A control system utilizing neural networks was developed for quadrotors; however, significant challenges were encountered in its implementation. In this decade, intelligent controllers have not been implemented in untethered trajectory-tracking flights.

Quadrotor control has gained significant attention from the general public, hobbyists, and researchers during this period, as shown in Figure 1. Open-source projects have emerged to support the educational and research advancements in quadrotors [62]. The use of quadrotors can be extended beyond traditional applications, with autonomous flights explored for artistic purposes [51], urban search and rescue missions [63], and industrial applications [52]. In addition, quadrotors have been employed in multi-agent systems [53], payload transportation [54], aerial manipulation [64], and high-speed flights [55], posing challenges in developing reliable trajectory generation and tracking control strategies. However, certain issues remain unresolved, including aerodynamics and proximity effects [56], precise modeling [65], actuator faults [66], and disturbances [67].

Similar to this section, a compilation of trendsetters across the world who authored the most popular papers was formed to establish a trend from early 2000s to 2013. However, determining the trends over the past decade (2014–2023) poses a challenge. Citation details for recently published papers, especially those published in the last five years, may not be reliable. The next section addresses this challenge by focusing on the identified trendsetters and searching for papers that present promising results and novel ideas for solving problems related to QTTC.

### 3. Data-Based Review of QTTC (2014—Present)

The objective of the trajectory-tracking controllers in this study is to design a controller that suffices two conditions: (1) bounding all closed-loop signals, including position, velocity, attitude, angular rates, and disturbance, and (2) ensuring the convergence of all tracking or estimation errors to a neighborhood of the origin, which can be made arbitrarily small. However, the design of such controllers encounters various negative factors that directly affect the quadrotor performance. For clarity, during the review process, this study excluded attitude-only controls (Figure 3).

This section provides a comprehensive review of the peer-reviewed tracking control literature from the past decade, encompassing an analysis of their modeling, control structures, and verification (Figure 5). Initially, 240 quadrotor trajectory-tracking controller proposals were collected. To facilitate the analysis, we selected 125 papers that were frequently cited, authored by trendsetters, presented interesting ideas, and included experimental verification. Furthermore, we analyzed the differences between high-impact and less-popular journals.

A majority of the published studies on quadrotor trajectory-tracking controllers have employed model-based approaches. We identified the four models used in these studies: Model A, which utilizes a simple Newton equation with  $F_N = T + mge_3$ ; Model B, which

considers aerodynamic forces  $F_N + F_{aero}$ ; Model C, which incorporates disturbances  $F_N + d$ ; and Model D, which combines all three components  $F_N + F_{aero} + d$ . In addition, some studies employed model-free approaches. Of the 240 papers reviewed, 67 utilized Model C and 77 employed Model D. These 144 papers proposed robust controllers, which is a popular topic in quadrotor control. However, after narrowing the database, we found that only 59 studies used Model C or D, and Model A emerged as the most commonly utilized model. Model-free controllers are gaining significant momentum due to the increasing popularity of controls based on reinforcement learning (RL).

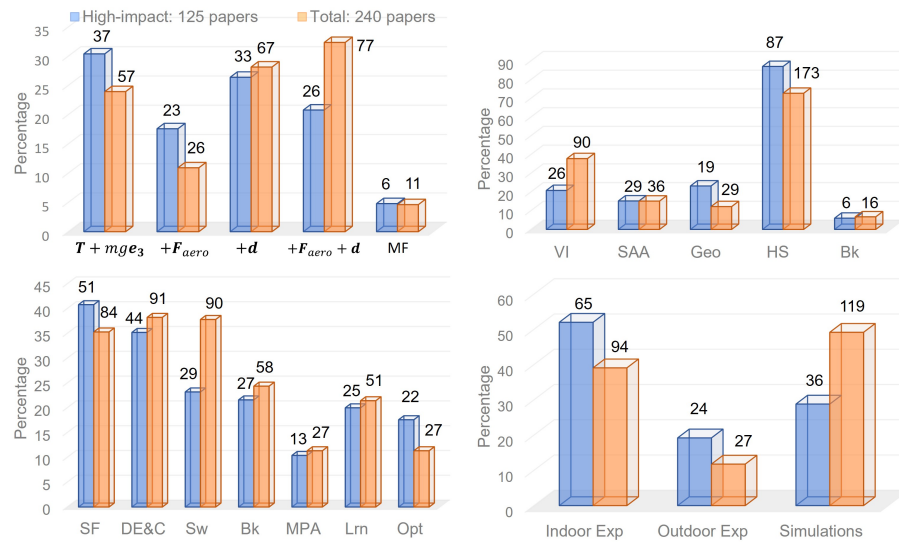


**Figure 5.** Comprehensive data-driven analysis: categorizing published studies into high-impact and lesser-known proposals, with statistical insights on modeling, control methods (CMs), coupling strategies, and verification methods.

We identified seven predominant solutions to quadrotor trajectory-tracking controller problems: simple feedback control (SF), disturbance estimation and compensation (DE&C), switching control (Sw), Bk, model parameter adaptation (MPA), Lrn, and Opt. The baseline controllers include SF, Sw, Bk, and Opt, which can be enhanced through the integration of the DE&C, MPA, and Lrn methodologies. Furthermore, Lrn can also serve as a baseline controller, as discussed in the latter part of this paper.

The SF encompasses PID control, state feedback, and other simple linear controllers that have been utilized in 84 of the 240 studies. Owing to their practicality and ease of tuning, they have gained high popularity in recent research and are the most preferred baseline controller in high-impact publications, with 40% utilization. It was observed that DE&C performed the best in both databases, at 38% and 35%, respectively. This is because it is moderately simple and can supplement any other baseline controller that is more robust against uncertainties and disturbances.

The Sw controllers, including SMC and RISE, are not preferred in high-impact journals but are popular in less popular ones. This is further explained in the next section. However, the prevalence of Opt controllers was higher in high-impact journals than in other journals.

In our investigation, we examined how published papers addressed the underactuation problem of quadrotors, as shown in Figure 5. We categorized them as follows: those using (7) and (10) were labeled as virtual inputs (VI), (6) as SAA, and (15) as the geometric approach (Geo). Despite the low preference in the 240-paper database, 65% (19 out of 29) of the Geo papers land on the high-impact list. Table 2 shows that agile flight solutions favor the geometric approach proposed by [46]. In addition, only 29% of the 90 papers that employed VI were included in the high-impact list. In both databases, most studies prefer a hierarchical structure (HS), either a position-attitude (PA), or a fully underactuated

cascaded control structure. Notably, some Bk proposed controllers that incorporated the VI to achieve the desired attitude angles.

**Table 2.** Experimental results comparison of published works on agile flight and MPC-based controllers.

Ref.	Yr	Ctt	Model	CM	Information	Ver	PS	m kg	max v <sub>a</sub>	Exp Con	Results	Github
[48]	11	2k+	▲▲	●	PA, Geo	◆	MC	0.5	3.6	HST	MTE 8	Maintained
[50]	11	390+	▲▲	●	MPC, N = 5	◆	MC	1.1	-	Line, wind	MTE 2.64	N/A
[57]	14	20+	▲▲▲	●	MPC, N = 8	◆	MC	0.65	1	Hel, fan P	-	[C1], Last 2016
[68]	15	100+	▲▲▲	●●	PA, Geo	◆	MC	0.76	1	Lissajous	-	[C2], Last 2022
[69]	16	120+	▲▲	●	MPC, N = 200, 2.2s	◆	MC	-	-	Outdoors	SD 13	[C3], Last 2018
[70]	16	280+	▲▲	●	PA, Geo	◆	Cam	0.25	5, 1.5 g	HST	-	N/A
[58]	17	190+	▲▲▲▲	●	MPC, N = 20, 2-s	◆	MC	3.42	-	HST, wind	RMSE 7.1	[C4], Last 2018
[71]	17	50+	▲▲▲	●	PA, Geo	◆	-	-	4	HST	RMSE 6.5	N/A
[72]	17	260+	▲▲▲	●	PA, Geo	◆	MC	0.61	5, 1.8 g	Lem	MTE 2.23	[C5], Last 2021
[73]	18	170+	▲▲	●	PA, Geo	◆	Cam	0.61	7	HST	-	[C6], Last 2023
[74]	18	40+	▲▲▲	●	PA, Geo	◆	Cam	-	15	HST	MTE 100	[C6], Last 2023
[75]	20	130+	▲▲▲	●	PA, VI	◆	Cam	-	12.9, 2.1 g	HST	RMSE 6.6	N/A
[76]	21	90+	▲▲	●	MPC, N = 20, 0.05-s	◆	MC	1	18, 4 g	HST	-	[C7], Last 2021
[77]	21	120+	▲▲	●●	MPC, N = 20, 0.05-s	◆	MC	1	12, 4 g	Lem	RMSE 2.4	[C8], Last 2021
[78]	21	40+	▲▲	●●	MPC, N = 20, 0.05-s	◆	MC	0.75	20, 4 g	HST	MTE 50	N/A
[79]	22	<10	▲▲▲▲	●●	PA, Geo	◆	MC	-	4	Cir, wind	RMSE 9	N/A
[80]	23	<10	▲▲	●	MPC, N = 8	◆	MC	1.1	5, 2 g	HST	MTE 8	N/A
[81]	23	<10	▲▲▲	●	MPC, shortest possible N	◆	MC	0.71	-	Cir	MTE 5	N/A
[82]	23	<10	▲▲▲	●	MPC, comp. of N	◆	LiDAR	1.5	5.86	HST	-	[C9], Last 2023
[83]	23	10+	-	●	RL, Gate Progress Objective	◆	MC	0.52	30, 12 g	HST	-	N/A

[C1] ntnu-arl/rmpc\_mav, [C2] fdcl-gwu/uav\_geometric, [C3] klaxalk/multirotor-control-board, [C4] ethz-asl/mav\_control\_rw, [C5] uzh-rpg/rpg\_quadrotor\_control/tree/master, [C6] Kumar-Robotics/kr\_autonomous\_flight, [C7] uzh-rpg/rpg\_time\_optimal, [C8] uzh-rpg/data\_driven\_mpc, [C9] hku-mars/IPC.

We analyzed the verification methods employed in these studies, which encompassed simulation-only, indoor, and outdoor experiments. Specifically, 121 of the reviewed studies conducted untethered experiments, whereas 119 relied solely on simulations, which indicates an identical distribution between the two methods. Notably, a significant proportion of the papers that underwent experimental validation were included in the high-impact list. Further, 24 of the 27 papers with outdoor experiments were included. However, we decided to exclude 29 papers with indoor experiments and 3 papers with outdoor experiments, owing to low citations or unsatisfactory results. We considered only recent papers without significant citation points to ensure a comprehensive evaluation.

In the next section, a detailed analysis of high-impact papers is presented with the objective of impartially identifying the most effective ones. To facilitate a fair comparison, we have organized the data in tables. The high-impact database was divided into several tables, allowing for a thorough and objective comparison based on the respective control objectives. In these tables, the publication year (Yr) and citation count (Ctt) are included to provide a clear timeline and help readers to determine the impact of each controller. Modeling is depicted as colored triangles, with  $F_N$  (▲▲),  $F_{aero}$  (▲), and  $d$  (▲). Control methods (CMs) are also indicated using colored circles, with SF (●), Sw (●), Bk (●), Lrn (●), and Opt (●). Verification methods are indicated by colored diamonds: simulation (◆), hardware-in-the-loop simulation (HILS) (◆), indoor experiments (◆), and outdoor experiments (◆). The PS includes motion capture (MC) systems, cameras (Cams), and GNSS. The experimental conditions included the trajectory followed and disturbance added for verification. Trajectories are shorthanded as high-speed trajectory (HST), circular (Cir), lemniscate (Lem), helical

(Hel), sinusoidal (Sine), square (Squ), or rectangular (Rec). The results are summarized as the tracking error in centimeters and type of tracking metric. The different tracking metrics used were the root-mean-square error (RMSE), maximum tracking error (MTE), mean absolute error (MAE), and standard deviation (SD). Braces denote the  $x$ ,  $y$ , and  $z$  tracking error while brackets represent different experimental conditions.

#### 4. Five Major Trends in the Last Decade

After collecting highly cited papers and those authored by the identified trend-setters, five major trends were observed. These trends are discussed in detail in the following subsections.

##### 4.1. Toward Agile Flight

Agile flight refers to a quadrotor's ability to execute rapid and precise maneuvers, encompassing quick changes in direction, high-speed maneuvers, and acrobatic flight. This capability offers numerous benefits and expands the potential applications of quadrotors in various domains such as drone racing, emergency response, and aerial acrobatics. One of the primary objectives of this research is to achieve precision control to execute agile maneuvers, where performance metrics such as tracking error, speed, and acceleration play a crucial role. Due to the high velocity of quadrotors during agile flights, obtaining accurate trajectory tracking becomes increasingly challenging. Furthermore, these performance metrics are affected by the quadrotor's characteristics, modeling, experimental conditions, and the type of position sensor (PS) used, as shown in Table 2. The agile flight work is highlighted in orange.

As a benchmark for agile flights, ref. [48] achieved a maximum position error of 8 cm using a 0.5 kg quadrotor that executes a high-velocity trajectory at 3.6 m/s. They identified the key constraints for agile flight, such as aerodynamic effects, power, and weight. Table 2 was created to facilitate a comprehensive comparison between proposals for agile flight, organizing important details that affect performance, including quadrotor mass, maximum speed, acceleration, experimental conditions, and results.

Lee et al. employed a combination of PD control and disturbance compensation to address aerodynamic effects and successfully achieved agile maneuvers using a 0.76 kg quadrotor [68].

$$T_1 = T + \beta(e_{\tilde{z}}, \dot{e}_{\tilde{z}})W_p \quad (16)$$

where  $T$  is from (14), and  $\beta(e_{\tilde{z}}, \dot{e}_{\tilde{z}})W_p$  accounts for the uncertainties. They demonstrated satisfactory results in tracking a Lissajous curve trajectory at speeds of up to 1 m/s.

In a separate study, Kumar's group designed a 0.25 kg quadrotor that is capable of aggressive flight, achieving velocities of up to 5 m/s, accelerations of up to 15 m/s<sup>2</sup>, and angular rotations of up to 800/s while navigating through narrow windows [70]. In this study, we set a new benchmark for control- and vision-based high-speed quadrotors using the position feedback obtained from an onboard single camera and an IMU. By incorporating simple lumped parameter models for induced drag and thrust into quadrotor dynamics, the trajectory-tracking error was significantly reduced to a maximum of 6.5 cm (a 75% decrease) from the original 26 cm [71].

$$T_2 = T - \omega_s RK_f R^\top v \quad (17)$$

where  $\omega_s = \sum_{i=1}^4 \omega_i$ . The aerodynamic force is modeled as  $F_{aero} = \omega_s RK_f R^\top v$ ; therefore, it is directly compensated. Hence, the identification of  $K_f$  is necessary. It should be noted that aerodynamic modeling and compensation have evolved from (1) to (8) to that used by [71].

A collaboration between the University of Zurich and Universite de Toulouse followed a similar approach. However, they utilized feedforward terms for body rates and angular

accelerations, resulting in improved trajectory tracking and the elimination of rotor speed ( $\omega_s$ ) dependency [72].

$$a_{fb} = -K_p e_{\xi} - K_d \dot{e}_{\xi} \quad (18)$$

$$a_{rd} = -R_d K_f R_d^{\top} \dot{\xi}_d \quad (19)$$

$$\tilde{a} = a_{fb} + a_d - a_{rd} + g e_3 \quad (20)$$

$$f_3 = \tilde{a} R_d e_3 + k_h v_h \quad (21)$$

where  $k_h$  is a constant,  $v_h = (v(x_b + y_b))^2$  is a quadratic velocity-dependent input disturbance, and  $[x_b, y_b, \chi_b]$  are orthogonal-direction vectors. It should be noted that aerodynamic effects are compensated for in two ways: one accounts for the effect of the quadrotor's movement, and the other compensates for the drag disturbance. The researchers achieved a maximum position error of 2.23 cm for a 0.61 kg quadrotor executing a lemniscate trajectory at speeds of up to 5 m/s. However, it is important to conduct an advanced identification of aerodynamic parameters through experiments for specific trajectories. It was observed that  $K_f = \text{diag}(k_{fx}, k_{fy}, 0)$  varies for each tested trajectory, where the circular trajectory yields  $\text{diag}(0.544, 0.386, 0)$  and the lemniscate trajectory results in  $\text{diag}(0.491, 0.0236, 0)$  at a speed of 2.8 m/s.

Kumar et al. surpassed previous velocity records, attaining a velocity of 7 m/s along a straight path in a GPS-denied environment [73]. In order to be eligible for the DARPA Fast Lightweight program, they developed a quadrotor from a DJI F450 frame that could fly at 18 m/s using only (21). However, during the testing, they operated below their maximum capability of 15 m/s. Even at this reduced speed, the quadrotor achieved an accuracy of less than a meter with drag compensation [74].

In [75], a group from MIT eliminated the modeling of aerodynamic drag used in previous studies [73,74]. Instead, they employed incremental nonlinear dynamic inversion (INDI) to track linear and angular accelerations robustly, even in the presence of aerodynamic drag.

$$T_4 = T_f - K_p e_{\xi} - K_d \dot{e}_{\xi} - (k_1 + 1)(a_f - \dot{\xi}_d) \quad (22)$$

where  $T_f$  and  $a_f$  are filtered signals from the INDI process. They achieved a velocity of 12.9 m/s and acceleration of 2.1 g, with a tracking error down to 6.6 cm RMSE during fast and successive turns. However, motor speed measurements are required for optical encoders.

Previously, agile flight primarily employed a PD control [46,48], as indicated in Table 2 and Equations (16) to (22). However, a group from the University of Zürich proposed an MPC in [76] that demonstrated superior performance compared to human expert drone pilots in a drone-racing task. To enhance their method, they introduced a data-driven MPC that is augmented with learned residual dynamics using a Gaussian process, thereby avoiding the need for tedious aerodynamic drag modeling [77]. Compared to [73], this new control scheme achieved a 16% increase in accuracy for velocities up to 12 m/s and accelerations beyond 4 g. The RMSE for tracking a circular trajectory was 31 cm for [76], 16.8 cm for [73], and 14.1 cm for [77]. Furthermore, the University of Zürich's group further improved their approach by adopting an  $\mathcal{L}_1$  adaptive technique to learn model uncertainties, including aerodynamic drag and unknown payloads [78]. During testing on a 20 m/s high-speed trajectory, it achieved a maximum position error of approximately 50 cm, whereas the non-adaptive case in [76] only achieved an accuracy of 1 m. In addition, in the simulations, the adaptive MPC outperformed [77].

Last year, [79,84] addressed the challenge of agile flying under wind disturbances by employing a wind velocity observer (WVO) for compensation. They separated the

aerodynamic drag term into two forces: one accounting for the effect of the quadrotor's movement and the other compensating for the wind velocity.

$$\begin{aligned} F_{aero} &= RK_f R^\top v + F_{w2} \\ T_5 &= T - RK_f R^\top v - \hat{F}_{w2} \end{aligned} \quad (23)$$

where  $F_{w2} = RK_f R^\top v_w$  and  $v_w$  are the estimated wind velocities obtained from WVO. They compared their method with that of [72], which indicated an error of 13 cm, while their approach achieved an error of 9 cm. The quadrotor flew at speeds of up to 4 m/s and was affected by a wind speed of 6 m/s.

In our observations, the geometric approach was utilized much more than the VI approach in agile flight, which was made popular by [48]. However, when the VI approach was used in [75], it yielded good performance.

The research group at the University of Zurich has created an open-source and open-hardware quadrotor platform designed for agile flight. The primary objective is to streamline research processes and empower practitioners to focus on fundamental challenges [85] (<https://github.com/uzh-rpg/agilicious>) (last accessed on 16 February 2024).

#### 4.2. Optimal Control

The model predictive control (MPC) is considered to be one of the best controllers for quadrotors, owing to its unique advantages and capabilities, especially in handling nonlinear and complex systems. By optimizing the control inputs over a prediction horizon  $N$ , MPC looks ahead, enabling the anticipation and accommodation of the quadrotor's future behavior. This facilitates agile flight. At each iteration, the following continuous nonlinear optimal control problem is solved.

$$\begin{aligned} \min \quad & J = \sum_{k=0}^{N-1} L(e_k, u_k) + M(e_N) \\ \text{s.t.} \quad & x_{k+1} = f(x_k, u_k) \quad \text{system model} \\ & x_0 = x(0) \quad \text{initial condition} \\ & x_k \in \mathcal{X} \quad \text{state constraints} \\ & u_k \in \mathcal{U} \quad \text{input constraints} \end{aligned} \quad (24)$$

where  $L(e_k, u_k)$  is the stage cost function with error  $e_k$  and input  $u_k$  variables, and  $M(e_N)$  is the terminal cost function. A noteworthy feature of MPC is the ability to incorporate various constraints, including physical limits on actuator commands, state constraints (e.g., position and velocity bounds), and obstacle avoidance constraints. This ensures that the quadrotor operates safely within its operational limits and avoids potential collisions. In addition, MPC allows for the simultaneous incorporation of multiple control objectives, such as optimizing energy consumption, minimizing tracking errors, and ensuring smooth motion.

Despite the advantages for quadrotor control, MPC has its own set of challenges, including being computationally demanding, moderately robust, and requiring advanced control algorithms to solve the optimization problem.

Although MPC inherently considers uncertainties and disturbances in the system during the optimization process, an MPC-controlled quadrotor is still susceptible to external disturbances, such as wind gusts or air turbulence. As a solution, an extension of [50] proposed a robust MPC designed to predict disturbance states and enhance robustness by considering eight constraints for the optimization problem [57]. A more advanced approach was presented in [58], wherein both linear and nonlinear MPC were designed in conjunction with an EKF-based external disturbance estimation. This led to the successful tracking of an aggressive trajectory, achieving a remarkable RMSE error of 10.8 cm and 7.1 cm for LMPC and NMPC, respectively. The disturbance estimation was fed back into the system dynamics, and the input constraints were imposed. This work was further

extended by [86], who added an additional soft constraint to the tracking error, as shown in (42), incurring only an additional 2.5 ms of computational cost.

The embedded MPC achieved a 200-step prediction horizon of over 2 s using 20 decision variables [69]. This extended prediction horizon is achieved by exponentially distributing the 20 decision variables throughout the prediction horizon, with the first 10 variables corresponding to the initial 10 control actions, followed by evenly spreading variables up to the 100th control action, which determines the control action for the last 100 steps. They demonstrated that a shorter prediction horizon could result in a higher chance of destabilization.

A group from the University of Zürich published major papers on MPC:

1. A time-optimal MPC aims to push the boundaries in agile flight, accomplishing a flight speed of 40 m/s. This model outperformed a human operator in a competitive drone-racing task [76]. The optimization problem is subject not only to the system dynamics, initial condition constraints, and input constraints but also to four additional constraints: progress evolution, boundary, sequence, and complimentary progress constraints. Despite using only 20 steps over 0.05 s, they consider the single-rotor thrust constraints rather than the four-dimensional continuous input space.
2. A data-driven MPC utilized a Gaussian process (GP) to model the aerodynamic effects in agile flight [77]. They used a multiple shooting scheme, divided the prediction horizon into a sequence of shorter intervals, and formulated the optimization problem over these intervals. However, the algorithm was not executed onboard, and commands were only sent from the ground station.
3. An adaptive MPC employs an  $\mathcal{L}_1$  adaptive augmentation to compensate for matched and unmatched uncertainties [78]. It surpassed the performance of [77] and was implemented on an onboard computer, specifically a Jetson TX2.
4. A policy-search-for-model-predictive-control framework consists of a parameterized MPC where the hard-to-optimize decision variables are represented as high-level policies. The quadrotor was shown to be agile enough to pass through swinging gates [87] ([https://github.com/uzh-rpg/high\\_mpc](https://github.com/uzh-rpg/high_mpc)) (last accessed on 16 February 2024).

An efficient NMPC, which solved the optimization problem using an improved C/GMRES algorithm, was proposed in [8]. This algorithm promises to reduce the computational complexity, specifically addressing the inequality constraint by imposing a penalty term on the cost function. However, the experimental results and analysis were underwhelming, as the quadrotor tracked a straight path at 0.1 m/s with difficult-to-evaluate accuracy.

More recently, a unified on-manifold MPC was proposed to overcome the issues of overparameterization or singularity by linearizing the system at each point along a trajectory under tracking [80]. First, the linearized system leads to an equivalent error system that maps the system state to local coordinates at each point along the reference trajectory. This results in a minimally parameterized, singularity-free MPC controller that is capable of tracking trajectories in the entire workspace. In their experiments with a DJI Manifold-2 controlled by an MPC with  $N = 8$  on the onboard computer, they compared their method with the NMPC of [58] and PD + drag compensation of [72] for quadrotors tracking a circular trajectory at 5 m/s. Based on the tracking error, they outperformed [72] by achieving an error of less than 10 cm compared to the latter's error of more than 10 cm. In addition, they claimed that [58] required a computation time of 10 ms, whereas it was 2 ms in the worst-case scenario. However, they did not compare their work with less computationally demanding [76] or more accurate and robust [78]. The same group proposed [82], where a linear MPC generates control actions within the safety constraints in 2 to 3.5 s. They have shown that MPC computation at 100 Hz improves the quadrotor's response speed to dynamic obstacles and disturbance rejection ability to external disturbances.

In [81], a computationally efficient NMPC was proposed to derive a growth-bound sequence, enabling the shortest possible prediction horizon for stability. A comparison

with [58] demonstrates that when [58] used  $N = 4$ , they failed, whereas their approach did not. They demonstrated a similar performance when  $N = 20$ , which was the value used by [58] in their verification. However, their work was not tested for aggressive trajectories under wind disturbances despite the promise made at the beginning of this paper.

#### 4.3. Learning-Based Control

Various Lrn techniques have been employed in quadrotor tracking control to address challenges such as disturbance estimation and identification of complex dynamics (see Section 4.5). In addition, some studies have explored the use of Lrn as a primary controller.

For instance, a type-2 fuzzy neural network (T2FNN) was used to improve PD control under high wind disturbances, achieving a 50% improvement from a 95.4 cm RMSE to a 52.0 cm RMSE.

The most cited paper in 2017 presented an RL-based method, particularly the deterministic policy gradient (DPG), which was introduced by a group at ETH, Zurich [88]. They used a linear MPC [58] as the baseline controller, with each time step taking approximately 1 ms in the simulations. Their indoor experiment with a hummingbird quadrotor following a square trajectory showed a relatively insignificant tracking error considering that it was a model-free control.

In [89], the authors demonstrated that a single neural network policy trained completely in a simulation for the task of recovery from harsh initial conditions can be generalized to multiple quadrotor platforms with unknown dynamic parameters. Their indoor setup achieved RMSE values of 19 and 47 cm for 33 g and 124 g quadrotors, respectively.

Another RL method was integrated with a disturbance compensator to achieve satisfactory tracking accuracy in outdoor environments, obtaining an RMSE of 45 cm while following a square trajectory [90].

The application of proximal policy optimization (PPO), a well-established continuous-space RL method, resulted in the quadrotor tracking of a circular pattern with an accuracy of 14.56 cm after 100,000 training episodes [91].

In [90], three approaches for implementing Deep DPG (DDPG) were presented: (1) using only instantaneous information, (2) allowing the agent to anticipate the curves, and (3) computing the optimal velocity according to the shape of the path. Following a lemniscate trajectory outdoors, Agent 1 achieved a 17.4 cm MAE, Agent 2 obtained an 11.4 cm MAE while maintaining a 0.91 m/s average velocity, and Agent 3 accomplished the task at a 1.63 m/s average velocity, resulting in a 16.8 cm MAE.

The research team from the University of Zurich conducted a comparative analysis between time-optimal MPC [76] and RL in the context of drone racing [83]. In this study, RL showcased the ability to fly up to 30 m/s by directly optimizing a task-level objective, enabling the discovery of a broader range of control responses that MPC cannot achieve. The limitation of MPC lies in its decomposition of the problem into planning and control, necessitating an intermediate representation such as a trajectory or path. This restriction imposes constraints on the expressiveness of control policies achievable by the system. In contrast, RL operates without the need for this decomposition or intermediate representation, eliminating constraints on the range of control policies. Additionally, RL can leverage domain randomization to enhance robustness, excelling at optimizing nonlinear, nonconvex, and even non-differentiable objectives. Unlike MPC, RL can optimize an objective such as the gate progress objective, directly maximizing progress toward the center of the next gate. The group also developed a vision-based RL algorithm for drone racing [92] and an imitation learning policy for high-speed flight in diverse natural environments, such as forests and steep snowy mountain terrains [93].

MPC, as the premier model-based controller, addresses safety and stability concerns inherent in RL-based methods. In [94], MPC manages control and obstacle avoidance, while RL guides the quadrotor through complex environments. In [95], a robust MPC method enhances safety margins compared to traditional RL methods. It employs a modified MPC algorithm that optimally balances cost minimization with aligning the neural network

policy, generating effective training data for improved policy training through standard supervised learning. On the other hand, RL can be used to solve the challenges of MPC, similar to [87,96], where the design of hard-to-engineer decision variables in MPC is efficiently addressed using a policy search algorithm.

Furthermore, another team has developed an open-source simulator that facilitates the comparison of different learning-based control methods with pre-existing PPO and soft actor–critic (SAC) codes [97] (<https://github.com/utiasDSL/safe-control-gym/tree/main/examples/rl/models/sac>) (last accessed on 16 February 2024).

#### 4.4. SMC and Bk Control Techniques

The most popular nonlinear strategies for quadrotor control are the Bk and SMC. These are both effective strategies for quadrotor control owing to their ability to handle highly nonlinear systems. Table 3 shows a comparison of Bk and SMC (with an Lrn controller, which is discussed later in this paper), with the most significant result being the tracking error. In experimental verification, most cases involve the introduction of some type of disturbance, such as wind disturbance, additional payload, or flying in an uncontrolled environment.

The Bk allows for the design of control laws for individual subsystems. This decoupling helps to address the underactuation problem in quadrotors. The asymptotic stability of the closed-loop system can be ensured during this process. For example, a three-step backstepping solution [98] is given by

$$\begin{aligned}
 \text{Step 1: } & \begin{cases} e_{\xi} = \xi - \xi_d, & \dot{e}_{\xi} = \dot{\xi} - \dot{\xi}_d \quad (\text{error 1}) \\ V_1 = 0.5e_{\xi}^T e_{\xi}, & \dot{V}_1 = e_{\xi}^T (\dot{\xi} - \dot{\xi}_d) \\ \dot{\xi}_c = \dot{e}_{\xi} - k_1 e_{\xi}, & \quad (\text{virtual control 1}) \end{cases} \\
 \text{Step 2: } & \begin{cases} \chi_1 = \dot{\xi} - \dot{\xi}_c - \delta, & \dot{\chi}_1 = \ddot{\xi} - \ddot{\xi}_d + k_1 \dot{e}_{\xi}, \quad (\text{error 2}) \\ V_2 = V_1 + 0.5\chi_1^T \chi_1, & \dot{V}_2 = \dot{V}_1 + \chi_1^T (T/m - \ddot{\xi}_d + k_1 \dot{e}_{\xi}) \\ \Pi = [f \quad \Omega_d]^T = B^+ (\Lambda - k_1 \chi_1), & \quad (\text{virtual control 2}) \end{cases} \\
 \text{Step 3: } & \begin{cases} e_{\Omega} = \Omega - \Omega_d, & \dot{e}_{\Omega} = \dot{\Omega} - \dot{\Omega}_d \quad (\text{error 3}) \\ V_3 = V_2 + 0.5e_{\Omega}^T e_{\Omega}, & \dot{V}_3 = \dot{V}_2 + e_{\Omega}^T (I^{-1} \tau_t - \dot{\Omega}_d) \\ \tau = -\Omega \times \Omega - \dot{\Omega}_d - K_3 e_{\Omega} + \beta, & \quad (\text{final control 2}) \end{cases}
 \end{aligned} \tag{25}$$

where  $B^+$  and  $\Lambda$  can be found in [99,100].  $\delta$  is a small arbitrary constant that is used to avoid certain singularities in the control input  $f$  based on Brockett's necessary condition [101]. In [102], additional Lyapunov functions were incorporated to introduce adaptive laws in order to estimate the mass, inertial tensor, and disturbance in the second and third steps of (25). Their results demonstrated a decreasing error of approximately 62 cm MTE and a 70% PI, which was the most promising in the MPA category, based on the collected data shown in Table 4. Furthermore, in [99], Xie et al. enhanced the three-step Bk control by complementing it with a Kalman–Bucy filter (DE&C and MPA). They achieved a significant improvement over their previous work, with a standard deviation (SD) of 5 cm, compared to 11 cm in [102].

**Table 3.** Experimental results comparison of published works on baseline controllers including backstepping-based, SMC-based, and learning-based controllers.

Ref.	Yr	Ctt	Model	CM, Gains	Ver	PS	m kg	Experiment Condition	Results, Code
[37]	07	1100+	▲▲▲	Integral Bk	◆	Cam	0.52	2-meter Sq	MTE, 20
[39]	07	420+	▲▲▲	PID	◆	GNSS	2.5	0.8-meter Sq	MTE, 50
[61]	07	<10	-	HOTSMC	◆	Cam	-	moving target	MAE, [8, 15, 13]
[103]	15	290+	▲▲▲	LPC	◆	GNSS	1.336	Point Tracking, unknown wind	-
[104]	15	170+	▲▲▲	RISE, 9	◆	Cam	0.0045	Rec(2.73 m, 0.2 m/s)	MTE [25, 50, 5]
[105]	16	160+	▲▲▲	T2FNN	◆	MC	0.68	Lem (3.2 m, 2 m/s)	RMSE 52.6
[88]	17	480+	MF	DPG	◆	MC	0.665	Squ (1 m)	[C10]
[89]	19	70+	MF	single policy RL	◆	MC	{0.033 0.124}	Lem (1 m)	MSE [19 47], [C11]
[106]	20	90+	▲▲▲	Bk-SMC, 12	◆	GNSS	2.5	predetermined	-
[91]	20	60+	MF	PPO	◆	MC	0.665	Cir (2 m)	RMSE 14.56, [C12]
[107]	20	20+	▲▲▲	STSMC, 20	◆	GNSS	2.5	Lem, Wind(3 m/s)	RMSE [21, 19, 16]
[98]	20	20+	▲▲▲	Sat Bk	◆	MC	0.2	Aggressive	-
[108]	21	20+	MF	DDPG	◆	GNSS	0.2	Hel, unknown wind	11.4
[109]	21	<10	▲▲▲	AFTSMC, 14	◆	GNSS	2.5	Cir (12 m)	RMSE [25, 22, 18]
[110]	22	20+	▲▲	NNMPC, 14	◆	MC	-	Sinusoidal	RMSE [16, 20, 8], [C13]
[111]	23	<10	▲▲	RISE + RL, 15	◆	MC	1.6	Smooth, unknown wind	MTE [10, 11, 5]

[C10] <https://bitbucket.org/leggedrobotics/rai/src/master/> (last accessed on 16 February 2024), [C11] [https://github.com/amolchanov86/quad\\_sim2multireal](https://github.com/amolchanov86/quad_sim2multireal) (last accessed on 16 February 2024), [C12] [https://github.com/anubhavparas/quadrotor\\_control\\_ppo](https://github.com/anubhavparas/quadrotor_control_ppo) (last accessed on 16 February 2024), [C13] [https://github.com/HKPolyU-UAV/airo\\_control\\_interface](https://github.com/HKPolyU-UAV/airo_control_interface) (last accessed on 16 February 2024).

Despite the popularity and usefulness of Bk control in quadrotor control, the inherent complexity of quadrotor dynamics leads to a challenging design process known as the “explosion of complexity”. Various solutions have been proposed to overcome this problem, including splitting the entire system into separate subsystems and using filters to obtain higher derivatives. For instance, altitude and yaw angle controllers were separated into control pairs x-pitch and y-roll, and an ultimate control was developed accordingly [112,113]. Alternatively, a hybrid hierarchical backstepping (HHB) control structure uses two separate backstepping approaches for both the translation and rotational dynamics, and coupling is performed using a virtual input in [12,114] and a geometric approach in [115].

On the other hand, dynamic surface control (DSC) is an extension of Bk control that replaces virtual control laws with a dynamic surface using filters, thus eliminating the need for differentiation of virtual control signals [10,12,114]. However, according to [116], the filtering error in the DSC may hamper the control quality. To address this issue, command-filter-based (CFB) [116] techniques, which filter the desired trajectories, have been proposed. Both the DSC and CFB methods use filtering techniques, which may sometimes be confusing. To clarify this, consider (25): DSC filters the virtual control  $\xi_c$ , whereas CFD filters  $\xi_d$ .

Two DSC proposals were authored by Zhang et al. and supplemented with fuzzy- and NN-based approximators in order to handle the unknown nonlinear part of the dynamic model [10,114]. They used digital filters for DSC and claimed that the control performance would be degraded or even become unstable when continuous-time control algorithms are used in the discrete-time controller. The digital 1-LPFs were utilized in every step to simplify the stability analysis.

$$\begin{aligned} \chi_{i,2d}(k) &= k_i \tilde{\chi}_{i,2}(k+1) + (1-k_i) \tilde{\chi}_{i,2}(k) \\ (\text{s.t.}) \quad \chi_{i,2d}(0) &= \tilde{\chi}_{i,2}(0), \quad i = 1, 2, 3 \end{aligned} \quad (26)$$

where  $\chi_{i,2d}(k)$  is the derivative of  $\chi_{i,1}(k)$  (i.e.,  $\dot{p}$  of  $p$ ), and  $\tilde{\chi}_{i,2}$  are the predicted signals. Both [10,114] demonstrated good performance in controlled environments, as shown in Table 4. Ref. [12] proposed a five-step approach from motor to position states and a similar filter as (26) in continuous form.

Usually, an accurate model is necessary for Bk control; however, a model-free integral Bk control was proposed in [117]. They presented a [4.34, 3.68, 223] cm RMSE, a 40%

improvement from a non-model-free one in the tracking performance for a 1.4 kg quadrotor. They estimated the unknown part of a dynamic model using an ultralocal model.

It is worth noting that the SMC dominates the 240-paper database, with 90 proposals. The SMC ensures stability even in the presence of disturbances through Lyapunov stability, although its performance depends on accurate modeling and gain tuning. Additional insights into SMC with adaptive options are available in the review paper [24]. Tuning the SMC gains involves two aspects: the gains of the sliding surface resembling PID gains and the gain of the switching control term. The latter can introduce chattering, which can be mitigated by various methods. High-order SMC [118,119] and super-twisting SMC (STSMC) [107,120] have been used to achieve faster convergence and reduced chattering compared with first-order SMC. Nonsingular types and smoothing functions, such as hyperbolic tangent functions, allow for smooth transitions between control modes and mitigate chattering [121]. In [109], the power-rate proportional reaching law ensured finite-time convergence with reduced chattering. In addition to addressing disturbances and uncertainties, modifications to the SMC have enabled global stability by ensuring the convergence of the system state to the sliding surface from any initial condition through the integral SMC [122] or global SMC [123]. TSMC [109,121,124] is a popular addition to achieve fast or fixed-time convergence. In a recent study, different types of continuous sliding surfaces were used [125].

A Bk-SMC hybrid approach presented in [106] proved to be superior to PID in outdoor experiments. However, there have been no qualitative analyses comparing this method with other methods. Other outdoor experiments were also conducted using STSMCM and adaptive fast TSMC (AFTSMC), which exhibited an RMSE tracking performance of less than 30 cm.

The RISE method combines Sw with DE by designing a switching control term to directly estimate and compensate for lumped disturbances [104,111,126]. Recently, RL was proposed in [111] to address the chattering issue in RISE, and it achieved a [10, 11, 5] cm MTE tracking performance.

#### 4.5. Supplementary Robust Techniques

Due to the inherent complexity and sensitivity of quadrotors to environmental factors, it is not surprising that researchers have proposed various supplementary robust techniques. Here, three sub-trends were summarized.

##### 4.5.1. Disturbance Estimation and Compensation

These methods serve as robust controllers that help to overcome external disturbances and modeling uncertainties. It was inferred that many studies consider these two factors as one entity, where their proposed approach can compensate for lumped disturbances. Therefore, disturbance estimation and compensation (DE&C) not only covers disturbance observers (DOBs) but also adaptive methods that estimate uncertainties only; however, the effects of the external disturbance can be included in that estimation and hence can be compensated as well.

Unlike agile flights, where researchers are aware of and can compare their results with those of previous studies, DE&C methods are much less organized and cannot be easily compared. One of the reasons might be that DE&C is only a supplementary controller (SpC), and the baseline controller (BsC), such as the PD control or SMC, has a more significant impact on the performance than DE&C. Therefore, a fairer comparison is not between different baseline controllers with DE&C, but between its baseline controller only and with DE&C using tracking error and additional control gains (ACGs) to verify the performance improvement by the specific DE&C. Furthermore, several factors can significantly affect the results, including the volume of disturbance given, quadrotor mass, and trajectory, as shown in Table 4. In addition, the number of ACGs is indicated to provide credit to proposals with fewer parameters to be tuned. A few studies that proposed the DE&C method are indicated in ■ in the SpC column.

**Table 4.** Experimental results comparison of published works with supplementary techniques using DE&C, MPA, and PPC.

Ref	Yr	Ctt	BsC	SpC	ACG	Ver	PS	m kg	Experiment Condition	Results	max PI
[126]	14	470+	●	■	+6	♦	-	1	Sinusoidal	MTE 10	-
[127]	14	200+	●	■	-	♦	MC	0.08	Lem (0.75 m)	MTE 7	-
[128]	14	110+	●	■	+3	♦	MC	0.65	Cir (0.9 m), Unknown m	-	-
[129]	15	230+	●	■	-	♦	MC	<1	Varying m, wind (5 m/s)	-	-
[130]	16	80+	●	■	+1	♦	MC	1.4	Squ (1 m)	RMSE [4.34, 3.68, 2.23]	40%
[131]	16	150+	●	■	+3	♦	GNSS	0.67	Squ (2 m), fan	MTE 20	-
[132]	16	100+	●	■	+1	♦	GNSS	0.67	Hov, wind (3.8 m/s), +52% m	MTE 15	-
[133]	17	140+	●	■	+6	♦	MC	1.4	Cir (1 m), fan	MTE [1.1, 1.6, 1.7]	75%
[134]	17	130+	●	■	+6	♦	GNSS	3	Rec (2 m), unknown wind	MTE [50, 50, 3]	-
[135]	17	60+	●	■	+6	♦	GNSS	2	cubic spline, unknown wind	-	-
[136]	17	30+	●	■	-	♦	GNSS	1.09	Hel (6 m), unknown wind	-	-
[137]	19	90+	●	■	-	♦	MC	1.75	Cir (1), Touch	MTE 3	77%
[86]	19	20+	●	■	+3	♦	MC	0.7	Line, wind (12 m/s)	MTE 10	74%
[138]	20	90+	●	■	+6	♦	MC	0.5	Cir, [(2 m, 1.26 m/s)]	MAE 3.5	77%
[10]	20	60+	●	■	+3	♦	MC	1.4	Hel	RMSE [2.28, 2.72, 0.97]	-
[139]	20	40+	●	■	+4	♦	MC	2.1	Sine, wind (10 m/s)	RMSE 7	53%
[9]	20	40+	●	■	+3	♦	Cam	0.063	Lissajous, fan	RMSE [5.8, 3.8, 2]	-
[140]	20	20+	●	■	+6	♦	MC	1.75	Sine, wind (1.5 m/s)	MTE [9.7, 16, 4.12]	-
[141]	20	10+	●	■	-	♦	GNSS	-	Lem (5 m), unknown wind	-	-
[124]	21	40+	●	■	-	♦	GNSS	0.38	Squ (4 m), no wind	RMSE [43, 42, 4]	-
[90]	21	20+	●	■	-	♦	GNSS	0.665	Squ (10 m), wind (4.2 m/s)	RMSE 45	44%
[142]	21	<10	●	■	+6	♦	GNSS	-	Circ, unknown wind	MTE 200	-
[143]	21	<10	●	■	-	♦	GNSS	1.346	Hel, unknown wind	MTE 56	41%
[114]	21	<10	●	■	-	♦	MC	1.4	Hel (0.6 m)	MTE [2.26, 2.04, 1.58]	-
[144]	22	10+	●	■	-	♦	GNSS	1.5	Cir (20 m), unknown wind	RMSE [25, 17, 16]	-
[145]	22	<10	●	■	+15	♦	MC	-	Sine, [+500g payload, wind (5 m/s)]	RMSE [7.5, 12.07, 9]	48%
[79]	22	<10	●	■	+3	♦	MC	-	Cir (5 m), wind (4 m/s)	RMSE 9.2	30%
[146]	22	<10	●	■	+4	♦	GNSS	2	Sine (2 m), unknown wind	[20, 20, 8]	67%
[147]	22	<10	●	■	+6	♦	MC	-	Lem, wind (2 m/s)	MAE [2.17, 1.11, 2.82]	-
[148]	22	<10	●	■	-	♦	GNSS	2.4	Cir, wind (3 m/s)	MAE [23, 26, 32]	-
[149]	22	<10	●	■	+4	♦	MC	1.79	Lem	RMSE [4.75, 3.3, 1.32]	-
[150]	23	<10	●	■	+30	♦	MC	0.25	Lem, [0.5 m, +60-g payload, wind]]	MAE [6.8, 3.97, 3.93]	-
[99]	23	<10	●	■	-	♦	MC	0.72	Lem, +0.045 kg payload	steady state error 5	55%

By using the data in Table 4, a number of papers have chosen to supplement PD control [46] using different approaches. The DE&C in [79,84] and the WVO in (23) are defined as

$$\begin{aligned}\dot{\chi}_1 &= \frac{1}{m}k_1\alpha\chi_1 + \frac{1}{m}(k_1\Lambda v + T_5 - \Lambda v + mge_3) \\ \hat{v}_w &= \chi_1 + k_1v\end{aligned}\quad (27)$$

where  $\alpha = RK_fR^\top$ . This decreased the MTE from 13 to 9 cm.

DE&C was applied to an agile flight as proposed by Lee et al. [68] and was designed as

$$\dot{\beta} = k_1(I_3 - \frac{\beta\beta^\top}{\beta^\top\beta})W_p(\dot{e}_\xi + k_2e_\xi)\quad (28)$$

Ref. [131] proposed an ESO-based robust compensator that can keep the position error less than 20 cm under 4.2 m/s wind for a hovering 0.67 kg quadrotor.

$$\begin{aligned}\dot{\chi}_1 &= k_1\chi_1 - k_1^2\chi_d + f/m - g \\ \dot{\chi}_2 &= k_1\chi_2 - 2k_1\chi_d + \chi_1 \\ \hat{d} &= mk_1^2(\chi_2 - \chi_d)\end{aligned}\quad (29)$$

where  $\chi_d$  is the desired altitude and  $\hat{d}$  is the estimated disturbance or robust compensating input that can be added to the baseline control input  $f$  to compensate for disturbances. However, no comparisons were made.

Ref. [133] proposed a DOB for attenuating disturbance force that can decrease the MTE from [5.44, 44, 6.69] cm to [1.1, 1.64, 1.77] cm for a QBall-X4 UAV following a circular trajectory and affected by a powerful electronic fan.

$$\begin{aligned}\dot{\chi}_1 &= \chi_1 - ge_3 + \frac{1}{m}fRe_3 \\ \dot{\chi}_2 &= k_1k_2\chi_2 + \ddot{\xi} - \dot{\chi}_1 + k_2(v - \chi_1) \\ \hat{d} &= mk_3\chi_2 + \ddot{\xi} - \dot{\chi}_1\end{aligned}\quad (30)$$

where  $4k_1k_2 > 1$  must be satisfied for asymptotic convergence of the disturbance estimation. It should be noted that [133] used a 3D approach for the PA structure, and [131] used a scalar approach for the FU structure.

Ref. [9] has proposed a UDE-based approach that can achieve [5.8, 3.8, 2] cm for a 63 g quadrotor following a Lissajous curve and being affected by 1.6 m/s wind.

$$\hat{d} = \mathcal{L}_1^{-1}((I_3 - G(s)^{-1})G(s)s) * \begin{bmatrix} e_{\xi} \\ \dot{e}_{\xi} \end{bmatrix} + \begin{bmatrix} \dot{e}_{\xi} \\ \ddot{\xi}_d \end{bmatrix}\quad (31)$$

where  $G(s)$  is a transfer function with three designable cut-off frequencies. A comparison was performed with another study but not with the baseline controller.

Ref. [140] has proposed a nonlinear DOB that is designed as

$$\begin{aligned}\dot{\chi}_1 &= -k_1(fRe_3 - mge_3 - m\ddot{\xi}_d + K_p e_{\xi} \\ &\quad + \hat{d}) + \dot{e}_{\xi} \\ \hat{d} &= \chi_1 + mk_1\dot{e}_{\xi}\end{aligned}\quad (32)$$

The performance results are presented in Table 4.

Ref. [138] proposed a multi-DOB (ESO + NDOB) that can surpass single-DOB implementation, where the baseline controller yielded a mean error of 15 cm, Base+ESO obtained 20.54 cm, Base+DO obtained 7.25 cm, and their proposed approach yielded 3.5 cm when a 0.5 kg quadrotor is following a circular trajectory at 1.26 m/s speed and being affected by hybrid disturbance (varying payload and wind disturbance). They concluded that ESO is not robust against varying payloads and worsens the performance. Thus, it has a higher error than the baseline controller, which will make other researchers disapprove. Their method combined the DOB by including the estimated disturbance in the estimation process.

DE&C can also supplement the SMC, where the estimated disturbance becomes the gain of the switching term to avoid tuning it [129].

$$\begin{aligned}\hat{d} &= Proj(d, -k_1 sign^T(\beta_a)\beta_a) \\ u^{SW} &= \hat{d}sign(\beta_a)\end{aligned}\quad (33)$$

where  $\beta_a$  is a function of  $e_{\xi}$  and  $Proj$  denotes a projection mechanism to ensure that  $\hat{d}$  is bounded over the compact set. The outdoor experiments showed very large tracking errors. In the most-cited paper in 2019 [151], online tuning of the upper bounds was proposed, but no experimental verification was provided.

Ref. [144] adopted a different approach and designed a nonlinear ESO to estimate the disturbances and then added it to the total control input. An outdoor experiment was conducted to obtain RMSE values of [24.5, 17.4, 16.3] cm. Their method was only compared with PID control, which resulted in a tracking error of 1.42 m and not with the baseline controller.

An adaptive Bk control that can estimate and compensate for lumped disturbances was proposed in [135]. However, no comparison was made with the baseline controller. In contrast, ref. [143] achieved a 56 cm MTE when the quadrotor was flying outdoors. They also reduced the tracking error by 41% for a spiral trajectory using a learning-based observer

to estimate the wind disturbance force. However, the hovering stability deteriorated due to the learning-based approach. In [146], a Bk controller was supplemented by GPIO, which improved the MTE from [60, 40, 15] cm to [20, 20, 8] cm for a 2 kg quadrotor following a sinusoidal trajectory with no disturbance. The readers are encouraged to check Table 4 to obtain summarized results of the other Bk proposals [127,128]. There have also been several proposals for Bk with other types of DOB, such as ESO [152] and NDOB [112,153], but there has been no experimental verification.

A PPO algorithm is combined with a nonlinear DOB, as shown below.

$$\hat{d} = mRa - fRe_3 + mge_3 \quad (34)$$

where  $a$  denotes the acceleration information obtained from the IMU. Their method improved the tracking error from [80, 46, 17] cm to [45, 41, 7] cm for a 0.665 kg quadrotor following a square trajectory outdoors with 4.2 m/s wind. Another approach uses neural networks (NNs) to estimate unknown lumped nonlinear functions [114,149,154,155]. In contrast, a learning-based observer has been used to estimate the wind disturbance force [139,141,143]. The NN method in [139] reduced the tracking error from 15 cm to 7 cm for a 2.1 kg quadrotor following a fast trajectory and being affected by wind (max of 10 m/s). In [141], a comparison was made between the baseline controller (LQR) and the neuro-fuzzy-based estimator, where it can be seen that the addition of their neuro-fuzzy-based estimator was better; however, no qualitative analysis was provided.

From Sec., the University of Zurich's group further improved their approach by adopting an  $\mathcal{L}_1$  adaptive MPC technique to compensate for both matched and unmatched disturbances.

$$\begin{aligned} \dot{\chi}_1 &= T_{MPC} + \gamma^m(u_m + d_m) + g^{um}d_{um} \\ \dot{\chi}_2 &= T_{MPC} + \gamma^m(u_m + \hat{d}_m) + g^{um}\hat{d}_{um} + k_1\tilde{\chi} \\ \dot{\tilde{\chi}} &= (\chi_2 - \chi_1) \end{aligned} \quad (35)$$

$$\begin{bmatrix} \hat{d}_m \\ \hat{d}_{um} \end{bmatrix} = I_3 \begin{bmatrix} \gamma^m \\ \gamma^{um} \end{bmatrix} k_1 (e^{k_1 T_s} - I_3) e^{k_1 T_s} \tilde{\chi}$$

The integration of the DE&C technique improved the tracking error by 85% for the 2.5 m/s trajectory and 77% for the 10 m/s trajectory.

In this section, we present various DE&C techniques applied to quadrotors. Based on the evaluation of the most promising DE&C techniques using the collected data, it was observed that [137,138] provided the highest percentage improvement (PI) of 77%, followed by [133] at 75%, and [86] at 74%. However, these techniques often exhibit similarities and have the potential for robust performance when appropriately calibrated and integrated into an accurate dynamic model. The best DE&C approach to employ hinges on the designer's proficiency and complexity of the tuning parameters, where [117] or [79,131] might emerge as superior choices. It is also admirable that the studies in [138,145,150] performed several tests to verify their method, which makes their method more convincing. For brevity, Table 4 contained the following shortcuts: \*Con1 = Cir, [(2 m, 1.26 m/s), swing payload, wind (5 m/s)] \*Con2 = Sine, [+500 g payload, wind (5 m/s)] \*Con3 = Lem, [0.5 m, +60 g payload, strong wind]).

#### 4.5.2. Adaptation, a Delicate Solution for Uncertainty

Obtaining an accurate mathematical model of a quadrotor is inherently challenging due to the uncertainties arising from the nonlinearity and complexity of the quadrotor system. In practical applications, such as aerial transportation or flight under wind conditions, the quadrotor control system must effectively cope with varying payloads and disturbances. The adaptive techniques offer a promising approach for enhancing quadrotor performance and robustness by continuously updating the control strategy or system parameters based on real-time feedback from sensors. These adaptive techniques can be classified into two categories: model parameter adaptation (MPA) for estimating unknown

parameters, such as  $K_f$  and  $m$ , and control parameter adaptation (CPA) for auto-tuning the control parameters to adapt to the real-time condition of the quadrotor.

The adaptation of lumped uncertainties can help to simplify the control problem. However, it may limit the flexibility of modeling owing to chunky compensation. The MPA and CPA, on the other hand, are more intricate because they address the robustness problem by surgically addressing the root causes of uncertainty [145]. As mentioned previously, aerodynamic parameters may vary depending on the trajectory and environment.

Similar to the previous topic, a fair comparison involves evaluating the baseline controller alone and comparing it with the inclusion of MPA using metrics such as the tracking error and other relevant parameters to quantify the performance improvement achieved by the specific MPA. Table 4 lists the works that proposed MPA methods, which are indicated as ■ in the SpC column.

The most-cited paper in 2014, ref. [126], focused on the immersion and invariance (I&I) parameter adaptation of the aerodynamic drag coefficient  $K_f$ . It demonstrates substantial improvements in a standard PD controller, reducing the maximum position error  $\|e_\zeta\|_\infty$  from  $\pm 0.5$  m to  $\pm 0.1$  m, when a 1 kg quadrotor follows a circular trajectory in a hardware-in-the-loop setup.

$$\hat{K}_f = k_1\beta_1(T + \beta_1(\hat{K}_f - \frac{1}{m}v\beta_2) + \beta_3) \quad (36)$$

where  $\beta_1 = \frac{1}{m}I_3v$ ,  $\beta_2 = \dot{e}_xi + K_p e_\zeta$ , and  $\beta_3 = K_p \dot{e}_xi - \ddot{\xi}_d$ .

A mass-adaptive technique with wind disturbance estimation and compensation (DE&C) is proposed for hovering Qball-X4, which carries an additional 350 g payload and is affected by a 3.8 m/s wind. The proposed method achieved maximum vertical and horizontal errors of 15 and 9 cm, respectively. It is worth noting that there was a significant difference in the performance between the simulation and experimental results. However, the most cited paper in 2018 [156] proposed an adaptive SMC that considers all parameters, including  $m$  and  $K_f$  (3). However, this study did not provide experimental validation.

In addition, ref. [102] proposed an adaptive Bk control technique that effectively handled both mass uncertainty and disturbances.

$$\begin{aligned} \dot{\hat{m}} &= k_1\chi_b^\top T \\ \dot{\hat{d}} &= k_2\chi_b \\ f &= Proj(\frac{1}{\hat{m}})e_3^\top(\hat{\Omega}\beta + T - Proj(\hat{d})) \end{aligned} \quad (37)$$

where  $\chi_b$  is the second error variable in the backstepping process and  $T$  is the PD control in (13). Based on a comprehensive theoretical framework, they achieved global uniformly ultimate boundedness (GUUB), even under uncertainties and disturbances. Although the parameters to be estimated are different, they compared their method with [126] and observed a decrease in the position error from 10 cm to 5 cm.

In [145], a three-tier robustness solution is proposed, which involves recursive least squares (RLS) adaptation for accurate parameter estimation  $\beta_1$ , gradient-type adaptation to improve transient performance  $\beta_2$ , and robust feedback to attenuate unmodeled uncertainties  $\beta_3$ . The control input is as follows:

$$T = -K_p e_\zeta - K_d \dot{e}_\zeta - \beta_1 - \beta_2 - \beta_3 \quad (38)$$

A comparative experiment was conducted to compare three control methods: (i) no utilization of  $\beta_1 = diag(\hat{m}, \hat{K}_f, \hat{d})$  (baseline controller), (ii) [140], and (iii) their full method under three different conditions: (i) no disturbance, (ii) with 500 g payload, and (iii) with 5 m/s wind disturbances. By using this notation, the proposed control achieved  $\|e_\zeta\|$  of 7.5, 12.07, 9 cm under the respective conditions. In comparison, the baseline controller achieved 10, 23, 13 cm and [140] achieved 9, 20, 12.5 cm. These results demonstrate that a delicate MPA can complement DE&C in order to achieve a better tracking performance.

Another adaptation technique is CPA, wherein the auto-tuning of control parameters is achieved during flight. In [136], a parameter-scheduled backstepping method was proposed, and experiments were conducted accordingly. Two parameter values, one for a milder controller and one for a more aggressive controller, are set and can be switched based on the current roll and pitch. The method was compared with PID, SMC, and a baseline controller in the experiments. However, no qualitative analysis was performed, and it was difficult to visually compare the results using the figures provided. Similarly, in [148], an auto-tuning SMC was proposed using a gradient-descent update law, and an outdoor experiment was conducted using a DJI M100. However, no qualitative analyses or comparative experiments have been conducted to demonstrate the effectiveness of the proposed approach.

#### 4.5.3. Prescribed Performance Control: Bounded Tracking Error

In our evaluation of various controls in agile flight, DE&C, and MPA, we employed tracking errors as the primary metric for performance comparison. However, some studies observed bounded tracking errors by imposing hard constraints. These methods are called prescribed performance controls (PPCs) and are listed in Table 4, where they are indicated by ■ in the SpC column.

A barrier Lyapunov function (BLF) can be used to constrain the tracking error.

$$u^{LBF} = \frac{e_{\xi}^{\bar{\xi}}}{k_1^2 - e_{\xi}^2} \quad (39)$$

where  $k_1$  is a set of tracking error bounds. This value approaches infinity when the tracking error  $e_{\xi}$  approaches  $k_1$ . Similarly, [140] used an LBF with another tuning parameter  $k_2$  to regulate the magnitude of the additional control term further.

$$u^{LBF} = k_2 \frac{e_{\xi}^{\bar{\xi}}}{k_1^2 - e_{\xi}^2} \quad (40)$$

Due to the sudden increase in the control input to constrain the position error, input saturation may occur. Hence, the authors emphasized the significance of appropriately choosing  $k_1$  and  $k_2$  to prevent saturation. Comparative experiments were conducted with PID and SMC but not with the baseline controller.

In [150], a barrier function that also approached infinity if the tracking error  $e_{\xi}$  approached the prescribed boundary was utilized. Unlike previous studies with constant constraints, this method employs a time-varying boundary constraint that gradually decreases until it reaches a preset value  $k_{\infty}$ , resulting in an increase in the tuning parameter.

$$\begin{aligned} \bar{e}_{\xi} &= I_3(\bar{k}_n - \bar{k}_{\infty})e^{-k_2 t} + \bar{k}_{\infty} \\ e_{\xi} &= I_3(\underline{k}_n - \underline{k}_{\infty})e^{-k_2 t} + \underline{k}_{\infty} \end{aligned} \quad (41)$$

where  $\underline{k}_n < e_{\xi}(0) < \bar{k}_n$ . Although there was no comparison with the baseline controller, three tests were conducted: (i) mass uncertainty, (ii) added payload, and (iii) wind disturbances. The results demonstrate that the tracking error  $e_{\xi}$  achieved values of 6.8, 3.97, 3.93 cm, all of which were within the prescribed boundary of  $\pm 15$  cm.

The aforementioned studies enforce a hard constraint that may counter the risk of infeasibility or saturation when a disturbance forces a tracking error to violate the constraints. An alternative approach is to implement a soft constraint within the MPC framework, wherein the slack variable  $k_2$  is added to the MPC output [86].

$$\begin{aligned} \bar{e}_{\xi} &\leq k_1 + k_2 \\ u^{MPC} &= [T \quad \phi_d \quad \theta_d \quad k_2] \end{aligned} \quad (42)$$

## 5. Comparative Discussion

Quadrotor control development typically involves four main steps to ensure the effectiveness and robustness of the controller: numerical simulation, controlled environment, uncontrolled environment, and actual deployment. In order to ascertain the current leading controller, it is informative to examine the developmental stage at which each controller is currently progressing.

Figure 6 shows the current situation of each controller based on the data presented in the previous section. A simple PD control can be complemented by DE&C, MPA, and/or PP techniques and can achieve small tracking errors even under uncertainties and disturbances, as shown in Table 4. The PD control provides a simple and solid foundation for integrating supplementary methods to address challenges in agile flight, robust flight, or robust agile flight scenarios. On the other hand, MPC is specifically accomplished in agile flights, where it is more difficult to obtain accurate trajectories. Furthermore, a group from the Czech Technical University deployed quadrotors with PD control [157] and MPC [158]. However, MPC faces the challenge of a heavy computational load, but there have been published ideas to tackle this issue [80,81]. The current focus is on transitioning these ideas from theoretical proposals to practical implementation in real flight scenarios while also addressing any potential challenges that may arise during this process. Upon the culmination of this comprehensive review, readers will be poised to deduce that both PD control and MPC possess the capacity to attain all control objectives. Consequently, these control methodologies are deemed more favorable within the realm of high-impact studies.

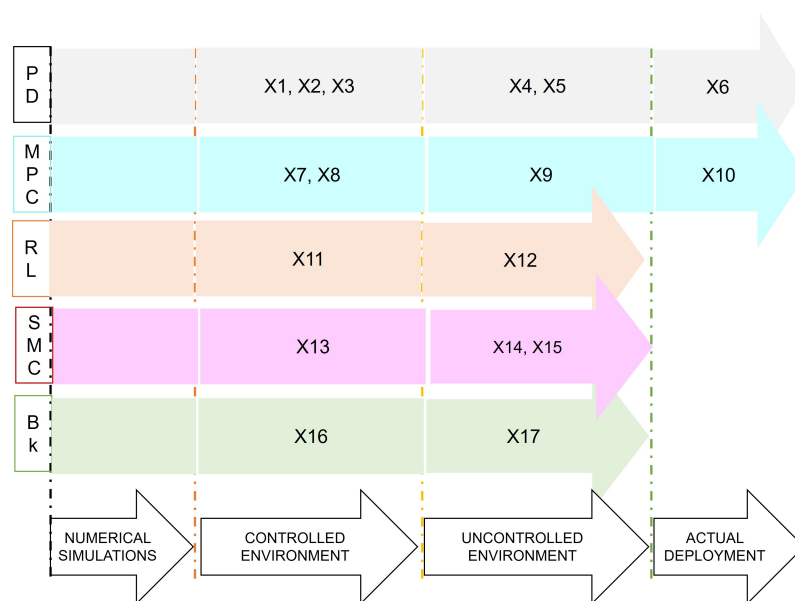


**Figure 6.** Illustration of the four development stages for quadrotor control leading to actual deployment. Reference numbers are as follows: [145] (X1), [75] (X2), [79] (X3), [15] (RP167), [74] (X5), [157] (X6), [80] (X7), [81] (X8), [110] (X9), [158] (X10), [83] (X11), [108] (X12), [149] (X13), [109] (X14), [144] (X15), [150] (X16), [148] (X17).

The Bk and SMC are both powerful control techniques with respective theoretical advantages, and they have already demonstrated good performance when tested outdoors. However, as shown in Figure 7, the Bk and SMC proposals have a low implementation rate compared to the PD and MPC techniques, which have been mostly implemented in experiments. None of the papers proposing Bk and SMC have made their implementation code available online. Additionally, they have not been applied to agile flights. Furthermore, it seems that the complexity outweighs the performance benefits. To reiterate their performance benefits, based on the collected data, in an indoor setup under strong winds, Bk+DE&C [150] achieved a tracking error of 3.93 cm MAE, outperforming PD+DE&C+MPA [145] with a tracking error of 9 cm RMSE. Similarly, in an outdoor setup,

Bk+DE&C [148] with [23, 26, 32] cm MAE and SMC+DE&C [144] with [25, 17, 16] cm RMSE outperformed PD+DE&C [134] with [50, 50, and 3] cm MTE. These arguments may not sound convincing because they are based on different qualitative metrics. Both the controllers face challenges in terms of actual deployment. A possible reason for this is that they require the design of multiple control laws and careful tuning of controller parameters. Practical engineers in the quadrotor industry may not possess sufficient expertise or understanding of these concepts, which makes it difficult to implement and tune these controllers. Moreover, troubleshooting them during the design process, which involves complex mathematical foundations, can be non-intuitive. The theoretical advantages of these controllers may transform into disadvantages when they must be understood and applied by industry professionals.

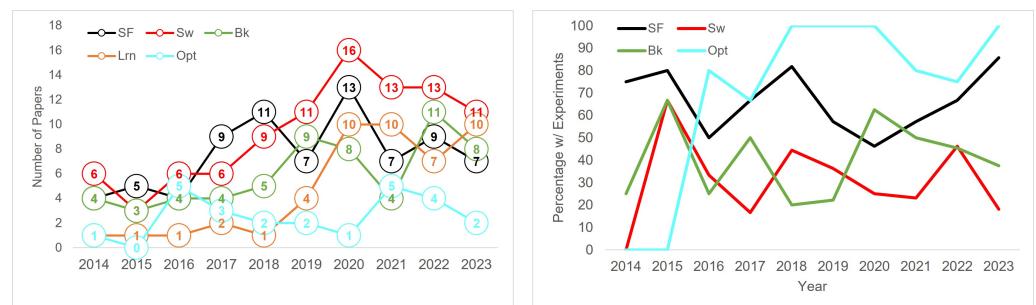


**Figure 7.** (Left) Year-by-year usage comparison of different controllers. (Right) Percentage of experimental papers per total usage for each controller, using the 240-paper database.

The Lrn has been increasingly adopted in quadrotor control because it offers potential advantages over traditional model-based control techniques. The DDPG method in [108] showed promising results, achieving an MAE of less than 15 cm in an outdoor setup, which has not been accomplished by model-based controllers according to the data that were gathered. However, safety concerns have arisen due to the unknown nature of this method. In addition, several bottlenecks, such as training complexity, data quality, and robustness, have inhibited its rise. In a workshop on “The Role of Robotics Simulators for Unmanned Aerial Vehicles” held at ICRA 2023 (<https://www.youtube.com/watch?v=MjqBZOVEL4c>) (last accessed on 16 February 2024), it was discussed that the problem of RL can be addressed by developing a good simulator for the RL to train as if in the real world or by recursively training until it becomes sufficiently better.

We have delved into the model selection process for each proposed method and observed that designers often choose their models based on personal discretion, with no discernible correlation to performance outcomes. Additionally, a notable trend indicates that high-impact publications are more inclined to include experimental verification.

## 6. Future Directions and Suggestions

The survey affirms that the field of QTTC has undergone extensive research. Within the QTTC scope, this survey specifically focuses on methodologies aimed at enhancing trajectory accuracy, improving robustness against system uncertainties and external disturbances, and achieving agile flights. These areas are identified as major trends with significant implications for overall performance. Additionally, the survey acknowledges research efforts in addressing challenges, including input saturation [153], actuator faults [155], sensor noise, time delays, global stability, safety concerns, and discretization issues [114].

Reflecting on historical insights, the first decade marked the challenge of developing untethered UAVs like OS4 quadrotors and STARMAC II. Despite more advanced controllers proposed in subsequent papers, the initial untethered quadrotors were controlled by simpler controllers like integral Bk control [37] with SAA and PID control [30]. Furthermore, two breakthroughs were the proposal of the geometric approach [46] and MPC [50], paving the way for new quadrotor capabilities like agile flight. In Section 4, we summarize the

next decade, highlighting five major trends. Agile flights were initially led by MPC and PD control with aerodynamic compensation. Recently, ref. [83] set a record, flying up to 30 m/s using RL-based control. Supplementary robust techniques, coupled with advanced controllers, enable a tracking accuracy of 1 cm in a controlled environment [133] and approximately 20 cm in an uncontrolled environment [146]. However, in [108], an RL-based approach achieved an MAE of less than 15 cm in an uncontrolled environment. We acknowledge that the tracking accuracy and flight speed are not only determined by QTTC but are also affected by other factors, such as motion planning, quadrotor vehicle parameters, sensor types, trajectory specifications, and environmental conditions.

Despite these achievements, studies reporting inferior or less remarkable results expose a discernible gap in the research field. Bridging this gap could redirect researchers' focus toward advancing the field. The following issues and suggestions are listed based on the information gathered.

- (a) Lack of standard for qualitative analysis: Some papers show promising results, but the majority of the published papers with experimental validation do not provide qualitative analysis, relying solely on performance figures for evaluation, as shown in Figure 8. This becomes challenging as accuracy is often evaluated in the order of a few centimeters.

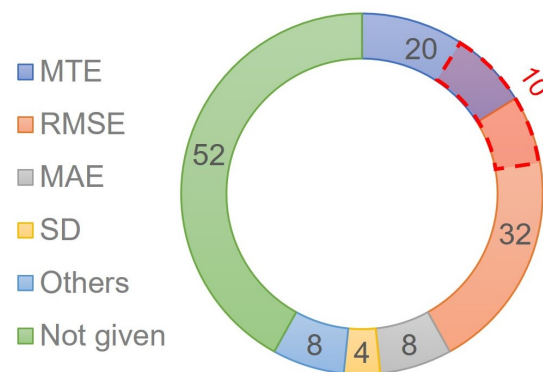


**Figure 8.** Variation in performance qualitative metrics across published works with experimental validation.

Complete qualitative analysis should include both RMSE and MTE to assess the performance and robustness of the control system. The RMSE represents the overall accuracy, while MTE captures the worst-case scenario of the trajectory-tracking task. According to those collected, only 10 papers [10,75,111,114,133,140,143,145,159,160] have presented both RMSE and MTE in their results, as shown in Figure 8.

- (b) Lack of standard for robustness evaluation: Despite gathering data to evaluate each proposal, it is difficult to determine which methods have good robustness characteristics. The main reason is that each paper verifies their method using different quadrotors and experiment conditions.

To address this issue, a standard for introducing disturbances and uncertainties based on quadrotor characteristics should be established. For instance, horizontal disturbance should be quantified in Newtons, relative to the drag-to-weight ratio,  $\rho_1 = \frac{d}{mg}$ , whereas payload  $m_p$  should be expressed as the ratio between total weight with the payload and the maximum thrust  $T_{max}$ ,  $\rho_2 = \frac{m_p}{T_{max}}$ .

- (c) Difficulty in reproducibility: Some papers do not disclose certain parameters, such as quadrotor mass, controller gains, wind disturbance speed, trajectory speed, controller frequency, position sensors, etc. This lack of transparency hinders the reproducibility of the paper, and this may prevent other researchers from building upon and improving the work. Another challenge in reproducibility is that one cannot guarantee that the results in Tables 2 and 3 can be obtained due to the inherent variability introduced by factors such as quadrotor vehicle parameters, sensor types, trajectory specifications,

and environmental conditions. While some researchers have proposed gain-tuning strategies for their method to enhance result reproducibility, it is noteworthy that the successful replication of outcomes is contingent upon the practitioner's proficiency in parameter tuning, introducing a significant dependency on individual tuning skills for achieving the promised performance.

One solution to these problems is providing an open-source implementation of their proposed controllers. This not only assists interested readers in replicating results for validation but also contributes to addressing potential issues. Utilizing platforms such as GitHub is highly advantageous, allowing interested individuals to engage in discussions, pose questions, and stay informed about the ongoing developments. This could also facilitate the transition of promising control technologies to actual deployment by addressing challenges.

In an ideal scenario, newly proposed controllers should undergo thorough qualitative and comparative analyses, employing metrics such as RMSE, MTE, and standardized robustness tests. The corresponding code should be made available online for both simulation and experimental setups, enabling reviewers and readers to replicate and verify the results.

Lastly, we present the following questions as statements for the future directions of QTTC.

1. Can MPC and PD control defend their status as the preferred controllers due to their promise of optimal performance and simplicity?
2. Will novel supplementary robust techniques aid existing or new control techniques in surpassing 15 cm accuracy and serve as platforms for applications requiring high accuracy?
3. Can SMC and Bk control demonstrate their worthiness and be deployed in actual deployment?
4. Will model-based control become obsolete as Lrn control introduces new capabilities in the future?

## 7. Conclusions

In this comprehensive review, we examined over 300 studies spanning two decades in the domain of quadrotor control with the aim of providing invaluable insights to aspiring early-career researchers. We revisited high-impact studies on quadrotor control conducted during the inaugural decade, offering a historical context for the current use of cutting-edge controllers. Subsequently, we dissected a 240-paper database from the subsequent decade, discerning the most promising and lagging controllers. A data-driven analysis that shed light on the decision-making processes of researchers, encompassing model selection, choice of control strategies, and verification methods, was conducted.

In order to unveil the five major trends in studies with substantial citations and/or authored by prominent groups, we conducted a qualitative analysis aimed at identifying the foremost candidates for implementation. PD control and MPC have emerged as prominent controllers and have already been successfully deployed. Supplementary robust techniques, including DE&C, MPA, and PPC, have enabled a tracking accuracy of 1 cm in a controlled environment and approximately 20 cm in an uncontrolled environment. On the other hand, RL-based techniques have proven to be game-changers, enabling a 30 m/s agile flight and less than 15 cm tracking accuracy for non-agile flight in an uncontrolled environment. Furthermore, conducting a comparative analysis proved challenging due to the absence of universally accepted performance standards and metrics. To address this gap, we present concrete recommendations for fostering collaborations to advance the future of quadrotor flights.

**Author Contributions:** Conceptualization, A.A.J. and S.S.; methodology, A.A.J.; formal analysis, A.A.J.; investigation, A.A.J.; resources, A.A.J. and S.S.; data curation, A.A.J. and S.S.; writing—original draft preparation, A.A.J.; writing—review and editing, A.A.J. and S.S.; visualization, A.A.J.; supervision, S.S.; project administration, S.S.; funding acquisition, S.S. All authors have read and agreed to the published version of the manuscript.

**Funding:** This paper is based on results obtained from a project, JPNP22002, commissioned by the New Energy and Industrial Technology Development Organization (NEDO).

**Data Availability Statement:** Publicly available datasets were analyzed in this study. This data can be found here: [https://docs.google.com/spreadsheets/d/e/2PACX-1vR70m8rMnMD2nDVaTxd5Yd4yi5IBrXbymaxukFoHsbJfl7aqq4DP0c15PnrMXnNpmWwTB\\_vs8I-UJxk/pubhtml](https://docs.google.com/spreadsheets/d/e/2PACX-1vR70m8rMnMD2nDVaTxd5Yd4yi5IBrXbymaxukFoHsbJfl7aqq4DP0c15PnrMXnNpmWwTB_vs8I-UJxk/pubhtml) (accessed on 16 February 2024). It has been published publicly, allowing everyone to access these datasets.

**Conflicts of Interest:** The authors declare no conflicts of interest.

## References

1. Grzonka, S.; Grisetti, G.; Burgard, W. A fully autonomous indoor quadrotor. *IEEE Trans. Robot.* **2011**, *28*, 90–100. [CrossRef]
2. Özbek, N.S.; Önkol, M.; Efe, M.Ö. Feedback control strategies for quadrotor-type aerial robots: A survey. *Trans. Inst. Meas. Control* **2016**, *38*, 529–554. [CrossRef]
3. Kendoul, F. Survey of advances in guidance, navigation, and control of unmanned rotorcraft systems. *J. Field Robot.* **2012**, *29*, 315–378. [CrossRef]
4. Mohsan, S.A.H.; Khan, M.A.; Noor, F.; Ullah, I.; Alsharif, M.H. Towards the unmanned aerial vehicles (UAVs): A comprehensive review. *Drones* **2022**, *6*, 147. [CrossRef]
5. Mu, C.; Zhang, Y. Learning-based robust tracking control of quadrotor with time-varying and coupling uncertainties. *IEEE Trans. Neural Netw. Learn. Syst.* **2019**, *31*, 259–273. [CrossRef] [PubMed]
6. Wang, N.; Deng, Q.; Xie, G.; Pan, X. Hybrid finite-time trajectory tracking control of a quadrotor. *ISA Trans.* **2019**, *90*, 278–286. [CrossRef] [PubMed]
7. Razmi, H.; Afshinfar, S. Neural network-based adaptive sliding mode control design for position and attitude control of a quadrotor UAV. *Aerosp. Sci. Technol.* **2019**, *91*, 12–27. [CrossRef]
8. Wang, D.; Pan, Q.; Shi, Y.; Hu, J.; Zhao, C. Efficient nonlinear model predictive control for quadrotor trajectory tracking: Algorithms and experiment. *IEEE Trans. Cybern.* **2021**, *51*, 5057–5068. [CrossRef] [PubMed]
9. Lu, Q.; Ren, B.; Parameswaran, S. Uncertainty and disturbance estimator-based global trajectory tracking control for a quadrotor. *IEEE/ASME Trans. Mechatron.* **2020**, *25*, 1519–1530. [CrossRef]
10. Zhang, X.; Wang, Y.; Zhu, G.; Chen, X.; Li, Z.; Wang, C.; Su, C.Y. Compound adaptive fuzzy quantized control for quadrotor and its experimental verification. *IEEE Trans. Cybern.* **2021**, *51*, 1121–1133. [CrossRef]
11. Han, H.; Cheng, J.; Xi, Z.; Yao, B. Cascade Flight Control of Quadrotors Based on Deep Reinforcement Learning. *IEEE Robot. Autom. Lett.* **2022**, *7*, 11134–11141. [CrossRef]
12. Wang, N.; Su, S.F.; Han, M.; Chen, W.H. Backpropagating constraints-based trajectory tracking control of a quadrotor with constrained actuator dynamics and complex unknowns. *IEEE Trans. Syst. Man. Cybern. Syst.* **2019**, *49*, 1322–1337. [CrossRef]
13. Yogi, S.C.; Behera, L.; Nahavandi, S. Adaptive Intelligent Minimum Parameter Singularity Free Sliding Mode Controller Design for Quadrotor. *IEEE Trans. Autom. Sci. Eng.* **2023**, *early access*. [CrossRef]
14. Wang, Z.; Zou, Y.; Liu, Y.; Meng, Z. Distributed control algorithm for leader–follower formation tracking of multiple quadrotors: Theory and experiment. *IEEE/ASME Trans. Mechatron.* **2020**, *26*, 1095–1105. [CrossRef]
15. Rinaldi, M.; Primatesta, S.; Guglieri, G. A comparative study for control of quadrotor uavs. *Appl. Sci.* **2023**, *13*, 3464. [CrossRef]
16. Maaruf, M.; Mahmoud, M.S.; Ma’arif, A. A survey of control methods for quadrotor uav. *Int. J. Robot. Control. Syst.* **2022**, *2*, 652–665. [CrossRef]
17. Zuo, Z.; Liu, C.; Han, Q.L.; Song, J. Unmanned aerial vehicles: Control methods and future challenges. *IEEE/CAA J. Autom. Sin.* **2022**, *9*, 601–614. [CrossRef]
18. Marshall, J.A.; Sun, W.; L’Afflito, A. A survey of guidance, navigation, and control systems for autonomous multi-rotor small unmanned aerial systems. *Annu. Rev. Control* **2021**, *52*, 390–427. [CrossRef]
19. Nguyen, H.T.; Quyen, T.V.; Nguyen, C.V.; Le, A.M.; Tran, H.T.; Nguyen, M.T. Control algorithms for UAVs: A comprehensive survey. *EAI Endorsed Trans. Ind. Netw. Intell. Syst.* **2020**, *7*, e5. [CrossRef]
20. Rubí, B.; Pérez, R.; Morcego, B. A survey of path following control strategies for UAVs focused on quadrotors. *J. Intell. Robot. Syst.* **2020**, *98*, 241–265. [CrossRef]
21. Kim, J.; Gadsden, S.A.; Wilkerson, S.A. A comprehensive survey of control strategies for autonomous quadrotors. *Can. J. Electr. Comput. Eng.* **2019**, *43*, 3–16. [CrossRef]
22. Nascimento, T.P.; Saska, M. Position and attitude control of multi-rotor aerial vehicles: A survey. *Annu. Rev. Control* **2019**, *48*, 129–146. [CrossRef]

23. Farid, G.; Hongwei, M.; Ali, S.M.; Liwei, Q. A review on linear and nonlinear control techniques for position and attitude control of a quadrotor. *Control Intell. Syst.* **2017**, *45*, 43–57.
24. L'afflitto, A.; Anderson, R.B.; Mohammadi, K. An introduction to nonlinear robust control for unmanned quadrotor aircraft: How to design control algorithms for quadrotors using sliding mode control and adaptive control techniques [focus on education]. *IEEE Control Syst. Mag.* **2018**, *38*, 102–121. [[CrossRef](#)]
25. Shraim, H.; Awada, A.; Youness, R. A survey on quadrotors: Configurations, modeling and identification, control, collision avoidance, fault diagnosis and tolerant control. *IEEE Aerosp. Electron. Syst. Mag.* **2018**, *33*, 14–33. [[CrossRef](#)]
26. Lee, H.; Kim, H.J. Trajectory tracking control of multirotors from modelling to experiments: A survey. *Int. J. Control Autom. Syst.* **2017**, *15*, 281–292. [[CrossRef](#)]
27. Chovancová, A.; Fico, T.; Hubinský, P.; Duchoň, F. Comparison of various quaternion-based control methods applied to quadrotor with disturbance observer and position estimator. *Robot. Auton. Syst.* **2016**, *79*, 87–98. [[CrossRef](#)]
28. Amin, R.; Aijun, L.; Shamshirband, S. A review of quadrotor UAV: Control methodologies and performance evaluation. *Int. J. Autom. Control* **2016**, *10*, 87–103. [[CrossRef](#)]
29. Zulu, A.; John, S. A review of control algorithms for autonomous quadrotors. *arXiv* **2016**, arXiv:1602.02622.
30. Hoffmann, G.; Huang, H.; Waslander, S.; Tomlin, C. Quadrotor helicopter flight dynamics and control: Theory and experiment. In Proceedings of the AIAA Guidance, Navigation and Control Conference and Exhibit, Honolulu, HI, USA, 18–21 August 2007; p. 6461.
31. Mistler, V.; Benallegue, A.; M'sirdi, N. Exact linearization and noninteracting control of a 4 rotors helicopter via dynamic feedback. In Proceedings of the 10th IEEE International Workshop on Robot and Human Interactive Communication. Roman 2001 (Cat. no. 01th8591), Bordeaux, Paris, France, 18–21 September 2001; pp. 586–593.
32. Altug, E.; Ostrowski, J.P.; Mahony, R. Control of a quadrotor helicopter using visual feedback. In Proceedings of the 2002 IEEE International Conference on Robotics and Automation (Cat. No. 02CH37292), Washington, DC, USA, 11–15 May 2002; Volume 1, pp. 72–77.
33. Hamel, T.; Mahony, R.; Lozano, R.; Ostrowski, J. Dynamic modelling and configuration stabilization for an X4-flyer. *IFAC Proc. Vol.* **2002**, *35*, 217–222. [[CrossRef](#)]
34. Bouabdallah, S.; Murrieri, P.; Siegwart, R. Design and control of an indoor micro quadrotor. In Proceedings of the IEEE International Conference on Robotics and Automation, 2004. Proceedings. ICRA'04, New Orleans, LA, USA, 26 April–1 May 2004; Volume 5, pp. 4393–4398.
35. Bouabdallah, S.; Noth, A.; Siegwart, R. PID vs. LQ control techniques applied to an indoor micro quadrotor. In Proceedings of the 2004 IEEE/RSJ International Conference on Intelligent Robots and Systems (IROS) (IEEE Cat. No. 04CH37566), Sendai, Japan, 28 September–2 October 2004; Volume 3, pp. 2451–2456.
36. Bouabdallah, S.; Siegwart, R. Backstepping and sliding-mode techniques applied to an indoor micro quadrotor. In Proceedings of the 2005 IEEE International Conference on Robotics and Automation, Barcelona, Spain, 18–22 April 2005; pp. 2247–2252.
37. Bouabdallah, S.; Siegwart, R. Full control of a quadrotor. In Proceedings of the 2007 IEEE/RSJ International Conference on Intelligent Robots and Systems, San Diego, CA, USA, 29 October–2 November 2007; pp. 153–158.
38. Adigbli, P.; Grand, C.; Mouret, J.B.; Doncieux, S. Nonlinear attitude and position control of a micro quadrotor using sliding mode and backstepping techniques. In Proceedings of the 7th European Micro Air Vehicle Conference (MAV07), Toulouse, France, 17–21 September 2007; pp. 1–9.
39. Hoffmann, G.; Waslander, S.; Tomlin, C. Quadrotor helicopter trajectory tracking control. In Proceedings of the AIAA Guidance, Navigation and Control Conference and Exhibit, Honolulu, HI, USA, 18–21 August 2008; p. 7410.
40. Huang, H.; Hoffmann, G.M.; Waslander, S.L.; Tomlin, C.J. Aerodynamics and control of autonomous quadrotor helicopters in aggressive maneuvering. In Proceedings of the 2009 IEEE International Conference on Robotics and Automation, Kobe, Japan, 12–17 May 2009; pp. 3277–3282.
41. Waslander, S.; Wang, C. Wind disturbance estimation and rejection for quadrotor position control. In Proceedings of the AIAA Infotech@ Aerospace Conference and AIAA Unmanned... Unlimited Conference, Seattle, WA, USA, 2009; p. 1983.
42. Madani, T.; Benallegue, A. Backstepping control for a quadrotor helicopter. In Proceedings of the 2006 IEEE/RSJ International Conference on Intelligent Robots and Systems, Beijing, China, 9–13 October 2006; pp. 3255–3260.
43. Madani, T.; Benallegue, A. Control of a quadrotor mini-helicopter via full state backstepping technique. In Proceedings of the 45th IEEE Conference on Decision and Control, San Diego, CA, USA, 13–15 December 2006; pp. 1515–1520.
44. Zuo, Z. Trajectory tracking control design with command-filtered compensation for a quadrotor. *IET Control Theory Appl.* **2010**, *4*, 2343–2355. [[CrossRef](#)]
45. Kendoul, F.; Yu, Z.; Nonami, K. Guidance and nonlinear control system for autonomous flight of minirotorcraft unmanned aerial vehicles. *J. Field Robot.* **2010**, *27*, 311–334. [[CrossRef](#)]
46. Lee, T.; Leok, M.; McClamroch, N.H. Geometric tracking control of a quadrotor UAV on SE (3). In Proceedings of the 49th IEEE Conference on Decision and Control (CDC), Atlanta, GA, USA, 5–17 December 2010; pp. 5420–5425.
47. Lee, T.; Leok, M.; McClamroch, N.H. Nonlinear robust tracking control of a quadrotor UAV on SE (3). *Asian J. Control* **2013**, *15*, 391–408. [[CrossRef](#)]
48. Mellinger, D.; Kumar, V. Minimum snap trajectory generation and control for quadrotors. In Proceedings of the 2011 IEEE International Conference on Robotics and Automation, Shanghai, China, 9–13 May 2011; pp. 2520–2525.

49. Mahony, R.; Kumar, V.; Corke, P. Multirotor aerial vehicles: Modeling, estimation, and control of quadrotor. *IEEE Robot. Autom. Mag.* **2012**, *19*, 20–32. [[CrossRef](#)]
50. Alexis, K.; Nikolakopoulos, G.; Tzes, A. Model predictive quadrotor control: Attitude, altitude and position experimental studies. *IET Control. Theory Appl.* **2012**, *6*, 1812–1827. [[CrossRef](#)]
51. Alonso-Mora, J.; Breitenmoser, A.; Rufli, M.; Siegwart, R.; Beardsley, P. Multi-robot system for artistic pattern formation. In Proceedings of the 2011 IEEE International Conference on Robotics and Automation, Shanghai, China, 9–13 May 2011; pp. 4512–4517.
52. Burri, M.; Nikolic, J.; Hürzeler, C.; Caprari, G.; Siegwart, R. Aerial service robots for visual inspection of thermal power plant boiler systems. In Proceedings of the 2012 2nd International Conference on Applied Robotics for the Power Industry (CARPI), Zurich, Switzerland, 11–13 September 2012; pp. 70–75.
53. Kushleyev, A.; Mellinger, D.; Powers, C.; Kumar, V. Towards a swarm of agile micro quadrotors. *Auton. Robot.* **2013**, *35*, 287–300. [[CrossRef](#)]
54. Sreenath, K.; Michael, N.; Kumar, V. Trajectory generation and control of a quadrotor with a cable-suspended load—a differentially-flat hybrid system. In Proceedings of the 2013 IEEE International Conference on Robotics and Automation, Karlsruhe, Germany, 6–10 May 2013; pp. 4888–4895.
55. Shen, S.; Mulgaonkar, Y.; Michael, N.; Kumar, V. Vision-Based State Estimation and Trajectory Control Towards High-Speed Flight with a Quadrotor. *Robot. Sci. Syst.* **2013**, *1*, 32.
56. Powers, C.; Mellinger, D.; Kushleyev, A.; Kothmann, B.; Kumar, V. Influence of aerodynamics and proximity effects in quadrotor flight. In Proceedings of the Experimental Robotics: The 13th International Symposium on Experimental Robotics, Québec City, QC, Canada, 18–21 June 2012; Springer: Berlin/Heidelberg, Germany, 2013; pp. 289–302.
57. Alexis, K.; Papachristos, C.; Siegwart, R.; Tzes, A. Robust explicit model predictive flight control of unmanned rotorcrafts: Design and experimental evaluation. In Proceedings of the 2014 European Control Conference (ECC), Strasbourg, France, 24–27 June 2014; pp. 498–503.
58. Kamel, M.; Burri, M.; Siegwart, R. Linear vs nonlinear mpc for trajectory tracking applied to rotary wing micro aerial vehicles. *IFAC-PapersOnLine* **2017**, *50*, 3463–3469. [[CrossRef](#)]
59. Xu, R.; Ozguner, U. Sliding mode control of a quadrotor helicopter. In Proceedings of the 45th IEEE Conference on Decision and Control, San Diego, CA, USA, 13–15 December 2006; pp. 4957–4962.
60. Lee, D.; Jin Kim, H.; Sastry, S. Feedback linearization vs. adaptive sliding mode control for a quadrotor helicopter. *Int. J. Control Autom. Syst.* **2009**, *7*, 419–428. [[CrossRef](#)]
61. Pham, H.T.; Dang, C.T.; Pham, T.B.; Truong, N.V. Hybrid Terminal Sliding Mode Control and quadrotor’s vision based ground object tracking. In Proceedings of the 2013 International Conference on Control, Automation and Information Sciences (ICCAIS), Nha Trang, Vietnam, 25–28 November 2013; pp. 334–340.
62. Lim, H.; Park, J.; Lee, D.; Kim, H.J. Build your own quadrotor: Open-source projects on unmanned aerial vehicles. *IEEE Robot. Autom. Mag.* **2012**, *19*, 33–45. [[CrossRef](#)]
63. Tomic, T.; Schmid, K.; Lutz, P.; Domel, A.; Kassecker, M.; Mair, E.; Grixia, I.L.; Ruess, F.; Suppa, M.; Burschka, D. Toward a fully autonomous UAV: Research platform for indoor and outdoor urban search and rescue. *IEEE Robot. Autom. Mag.* **2012**, *19*, 46–56. [[CrossRef](#)]
64. Scholten, J.L.; Fumagalli, M.; Stramigioli, S.; Carloni, R. Interaction control of an UAV endowed with a manipulator. In Proceedings of the 2013 IEEE International Conference on Robotics and Automation, Karlsruhe, Germany, 6–10 May 2013; pp. 4910–4915.
65. Sa, I.; Corke, P. System identification, estimation and control for a cost effective open-source quadcopter. In Proceedings of the 2012 IEEE International Conference on Robotics and Automation, St Paul, MI, USA, 14–18 May 2012; pp. 2202–2209.
66. Mueller, M.W.; D’Andrea, R. Stability and control of a quadcopter despite the complete loss of one, two, or three propellers. In Proceedings of the 2014 IEEE International Conference on Robotics and Automation (ICRA), Hong Kong, China, 31 May–7 June 2014; pp. 45–52.
67. Escareño, J.; Salazar, S.; Romero, H.; Lozano, R. Trajectory control of a quadrotor subject to 2D wind disturbances: Robust-adaptive approach. *J. Intell. Robot. Syst.* **2013**, *70*, 51–63. [[CrossRef](#)]
68. Goodarzi, F.A.; Lee, D.; Lee, T. Geometric adaptive tracking control of a quadrotor unmanned aerial vehicle on SE (3) for agile maneuvers. *J. Dyn. Syst. Meas. Control* **2015**, *137*, 091007. [[CrossRef](#)]
69. Baca, T.; Loianno, G.; Saska, M. Embedded model predictive control of unmanned micro aerial vehicles. In Proceedings of the 2016 21st International Conference on Methods and Models in Automation and Robotics (MMAR), Miedzyzdroje, Poland, 29 August–1 September 2016; pp. 992–997.
70. Loianno, G.; Brunner, C.; McGrath, G.; Kumar, V. Estimation, control, and planning for aggressive flight with a small quadrotor with a single camera and IMU. *IEEE Robot. Autom. Lett.* **2016**, *2*, 404–411. [[CrossRef](#)]
71. Svacha, J.; Mohta, K.; Kumar, V. Improving quadrotor trajectory tracking by compensating for aerodynamic effects. In Proceedings of the 2017 International Conference on Unmanned Aircraft Systems (ICUAS), Miami, FL, USA, 13–16 June 2017; pp. 860–866.
72. Faessler, M.; Franchi, A.; Scaramuzza, D. Differential flatness of quadrotor dynamics subject to rotor drag for accurate tracking of high-speed trajectories. *IEEE Robot. Autom. Lett.* **2018**, *3*, 620–626. [[CrossRef](#)]

73. Mohta, K.; Watterson, M.; Mulgaonkar, Y.; Liu, S.; Qu, C.; Makineni, A.; Saulnier, K.; Sun, K.; Zhu, A.; Delmerico, J.; et al. Fast, autonomous flight in GPS-denied and cluttered environments. *J. Field Robot.* **2018**, *35*, 101–120. [[CrossRef](#)]
74. Mohta, K.; Sun, K.; Liu, S.; Watterson, M.; Pfrommer, B.; Svacha, J.; Mulgaonkar, Y.; Taylor, C.J.; Kumar, V. Experiments in fast, autonomous, gps-denied quadrotor flight. In Proceedings of the 2018 IEEE International Conference on Robotics and Automation (ICRA), Brisbane, Australia, 21–25 May 2018; pp. 7832–7839.
75. Tal, E.; Karaman, S. Accurate tracking of aggressive quadrotor trajectories using incremental nonlinear dynamic inversion and differential flatness. *IEEE Trans. Control. Syst. Technol.* **2020**, *29*, 1203–1218. [[CrossRef](#)]
76. Foehn, P.; Romero, A.; Scaramuzza, D. Time-optimal planning for quadrotor waypoint flight. *Sci. Robot.* **2021**, *6*, eabh1221. [[CrossRef](#)] [[PubMed](#)]
77. Torrente, G.; Kaufmann, E.; Föhn, P.; Scaramuzza, D. Data-driven MPC for quadrotors. *IEEE Robot. Autom. Lett.* **2021**, *6*, 3769–3776. [[CrossRef](#)]
78. Hanover, D.; Foehn, P.; Sun, S.; Kaufmann, E.; Scaramuzza, D. Performance, precision, and payloads: Adaptive nonlinear mpc for quadrotors. *IEEE Robot. Autom. Lett.* **2021**, *7*, 690–697. [[CrossRef](#)]
79. Jia, J.; Guo, K.; Yu, X.; Zhao, W.; Guo, L. Accurate high-maneuvering trajectory tracking for quadrotors: A drag utilization method. *IEEE Robot. Autom. Lett.* **2022**, *7*, 6966–6973. [[CrossRef](#)]
80. Lu, G.; Xu, W.; Zhang, F. On-manifold model predictive control for trajectory tracking on robotic systems. *IEEE Trans. Ind. Electron.* **2022**, *70*, 9192–9202. [[CrossRef](#)]
81. Gomaa, M.A.; De Silva, O.; Mann, G.K.; Gosine, R.G. Computationally Efficient Stability-Based Nonlinear Model Predictive Control Design for Quadrotor Aerial Vehicles. *IEEE Trans. Control Syst. Technol.* **2022**, *31*, 615–630. [[CrossRef](#)]
82. Liu, W.; Ren, Y.; Zhang, F. Integrated Planning and Control for Quadrotor Navigation in Presence of Suddenly Appearing Objects and Disturbances. *IEEE Robot. Autom. Lett.* **2023**, *9*, 899–906. [[CrossRef](#)]
83. Song, Y.; Romero, A.; Müller, M.; Koltun, V.; Scaramuzza, D. Reaching the limit in autonomous racing: Optimal control versus reinforcement learning. *Sci. Robot.* **2023**, *8*, eadg1462. [[CrossRef](#)]
84. Jia, J.; Guo, K.; Yu, X.; Guo, L.; Xie, L. Agile flight control under multiple disturbances for quadrotor: Algorithms and evaluation. *IEEE Trans. Aerosp. Electron. Syst.* **2022**, *58*, 3049–3062. [[CrossRef](#)]
85. Foehn, P.; Kaufmann, E.; Romero, A.; Penicka, R.; Sun, S.; Bauersfeld, L.; Laengle, T.; Cioffi, G.; Song, Y.; Loquercio, A.; et al. Agilicious: Open-source and open-hardware agile quadrotor for vision-based flight. *Sci. Robot.* **2022**, *7*, eabl6259. [[CrossRef](#)]
86. Hentzen, D.; Stastny, T.; Siegwart, R.; Brockers, R. Disturbance estimation and rejection for high-precision multirotor position control. In Proceedings of the 2019 IEEE/RSJ International Conference on Intelligent Robots and Systems (IROS), Macau, China, 3–8 November 2019; pp. 2797–2804.
87. Song, Y.; Scaramuzza, D. Policy search for model predictive control with application to agile drone flight. *IEEE Trans. Robot.* **2022**, *38*, 2114–2130. [[CrossRef](#)]
88. Hwangbo, J.; Sa, I.; Siegwart, R.; Hutter, M. Control of a quadrotor with reinforcement learning. *IEEE Robot. Autom. Lett.* **2017**, *2*, 2096–2103. [[CrossRef](#)]
89. Molchanov, A.; Chen, T.; Hönig, W.; Preiss, J.A.; Ayanian, N.; Sukhatme, G.S. Sim-to-(multi)-real: Transfer of low-level robust control policies to multiple quadrotors. In Proceedings of the 2019 IEEE/RSJ International Conference on Intelligent Robots and Systems (IROS), Macau, China, 3–8 November 2019; pp. 59–66.
90. Pi, C.H.; Ye, W.Y.; Cheng, S. Robust quadrotor control through reinforcement learning with disturbance compensation. *Appl. Sci.* **2021**, *11*, 3257. [[CrossRef](#)]
91. Pi, C.H.; Hu, K.C.; Cheng, S.; Wu, I.C. Low-level autonomous control and tracking of quadrotor using reinforcement learning. *Control Eng. Pract.* **2020**, *95*, 104222. [[CrossRef](#)]
92. Fu, J.; Song, Y.; Wu, Y.; Yu, F.; Scaramuzza, D. Learning deep sensorimotor policies for vision-based autonomous drone racing. *arXiv* **2022**, arXiv:2210.14985.
93. Loquercio, A.; Kaufmann, E.; Ranftl, R.; Müller, M.; Koltun, V.; Scaramuzza, D. Learning high-speed flight in the wild. *Sci. Robot.* **2021**, *6*, eabg5810. [[CrossRef](#)] [[PubMed](#)]
94. Greatwood, C.; Richards, A.G. Reinforcement learning and model predictive control for robust embedded quadrotor guidance and control. *Auton. Robot.* **2019**, *43*, 1681–1693. [[CrossRef](#)]
95. Zhang, T.; Kahn, G.; Levine, S.; Abbeel, P. Learning deep control policies for autonomous aerial vehicles with mpc-guided policy search. In Proceedings of the 2016 IEEE International Conference on Robotics and Automation (ICRA), Stockholm, Sweden, 16–21 May 2016; pp. 528–535.
96. Song, Y.; Scaramuzza, D. Learning high-level policies for model predictive control. In Proceedings of the 2020 IEEE/RSJ International Conference on Intelligent Robots and Systems (IROS), Las Vegas, NV, USA, 25–29 October 2020; pp. 7629–7636.
97. Yuan, Z.; Hall, A.W.; Zhou, S.; Brunke, L.; Greeff, M.; Panerati, J.; Schoellig, A.P. Safe-control-Gym: A unified benchmark suite for safe learning-based control and reinforcement learning in robotics. *IEEE Robot. Autom. Lett.* **2022**, *7*, 11142–11149. [[CrossRef](#)]
98. Xie, W.; Yu, G.; Cabecinhas, D.; Cunha, R.; Silvestre, C. Global saturated tracking control of a quadcopter with experimental validation. *IEEE Control Syst. Lett.* **2020**, *5*, 169–174. [[CrossRef](#)]
99. Zhu, X.Z.; Cabecinhas, D.; Xie, W.; Casau, P.; Silvestre, C.; Batista, P.; Oliveira, P. Kalman–Bucy filter-based tracking controller design and experimental validations for a quadcopter with parametric uncertainties and disturbances. *Int. J. Syst. Sci.* **2023**, *54*, 17–41. [[CrossRef](#)]

100. Aguiar, A.P.; Hespanha, J.P. Trajectory-tracking and path-following of underactuated autonomous vehicles with parametric modeling uncertainty. *IEEE Trans. Autom. Control* **2007**, *52*, 1362–1379. [[CrossRef](#)]
101. Rw, B. Asymptotic Stability and Feedback Stabilization, Differential Geometric Control Theory. *Birkhauser* **1983**, *181*, 181–191.
102. Xie, W.; Cabecinhas, D.; Cunha, R.; Silvestre, C. Adaptive backstepping control of a quadcopter with uncertain vehicle mass, moment of inertia, and disturbances. *IEEE Trans. Ind. Electron.* **2022**, *69*, 549–559. [[CrossRef](#)]
103. Choi, Y.C.; Ahn, H.S. Nonlinear control of quadrotor for point tracking: Actual implementation and experimental tests. *IEEE/ASME Trans. Mechatron.* **2015**, *20*, 1179–1192. [[CrossRef](#)]
104. Zhang, X.; Xian, B.; Zhao, B.; Zhang, Y. Autonomous flight control of a nano quadrotor helicopter in a GPS-denied environment using on-board vision. *IEEE Trans. Ind. Electron.* **2015**, *62*, 6392–6403. [[CrossRef](#)]
105. Kayacan, E.; Maslim, R. Type-2 fuzzy logic trajectory tracking control of quadrotor VTOL aircraft with elliptic membership functions. *IEEE/ASME Trans. Mechatron.* **2016**, *22*, 339–348. [[CrossRef](#)]
106. Xu, L.X.; Ma, H.J.; Guo, D.; Xie, A.H.; Song, D.L. Backstepping sliding-mode and cascade active disturbance rejection control for a quadrotor UAV. *IEEE/ASME Trans. Mechatron.* **2020**, *25*, 2743–2753. [[CrossRef](#)]
107. Tripathi, V.K.; Kamath, A.K.; Behera, L.; Verma, N.K.; Nahavandi, S. Finite-time super twisting sliding mode controller based on higher-order sliding mode observer for real-time trajectory tracking of a quadrotor. *IET Control Theory Appl.* **2020**, *14*, 2359–2371. [[CrossRef](#)]
108. Rubí, B.; Morcego, B.; Pérez, R. Deep reinforcement learning for quadrotor path following with adaptive velocity. *Auton. Robot.* **2021**, *45*, 119–134. [[CrossRef](#)]
109. Tripathi, V.K.; Kamath, A.K.; Behera, L.; Verma, N.K.; Nahavandi, S. An adaptive fast terminal sliding-mode controller with power rate proportional reaching law for quadrotor position and altitude tracking. *IEEE Trans. Syst. Man. Cybern. Syst.* **2022**, *52*, 3612–3625. [[CrossRef](#)]
110. Jiang, B.; Li, B.; Zhou, W.; Lo, L.Y.; Chen, C.K.; Wen, C.Y. Neural network based model predictive control for a quadrotor UAV. *Aerospace* **2022**, *9*, 460. [[CrossRef](#)]
111. Hua, H.; Fang, Y. A Novel Reinforcement Learning-Based Robust Control Strategy for a Quadrotor. *IEEE Trans. Ind. Electron.* **2023**, *70*, 2812–2821. [[CrossRef](#)]
112. Chen, F.; Lei, W.; Zhang, K.; Tao, G.; Jiang, B. A novel nonlinear resilient control for a quadrotor UAV via backstepping control and nonlinear disturbance observer. *Nonlinear Dyn.* **2016**, *85*, 1281–1295. [[CrossRef](#)]
113. Ramirez-Rodriguez, H.; Parra-Vega, V.; Sanchez-Orta, A.; Garcia-Salazar, O. Robust backstepping control based on integral sliding modes for tracking of quadrotors. *J. Intell. Robot. Syst.* **2014**, *73*, 51–66. [[CrossRef](#)]
114. Zhang, X.; Wang, Y.; Zhu, G.; Chen, X.; Su, C.Y. Discrete-time adaptive neural tracking control and its experiments for quadrotor unmanned aerial vehicle systems. *IEEE/ASME Trans. Mechatron.* **2023**, *28*, 1201–1212. [[CrossRef](#)]
115. Jiang, T.; Lin, D.; Song, T. Finite-time backstepping control for quadrotors with disturbances and input constraints. *IEEE Access* **2018**, *6*, 62037–62049. [[CrossRef](#)]
116. Liu, K.; Wang, R. Antisaturation command filtered backstepping control-based disturbance rejection for a quadrotor UAV. *IEEE Trans. Circuits Syst. II Express Briefs* **2021**, *68*, 3577–3581. [[CrossRef](#)]
117. Younes, Y.A.; Drak, A.; Noura, H.; Rabhi, A.; Hajjaji, A.E. Robust model-free control applied to a quadrotor UAV. *J. Intell. Robot. Syst.* **2016**, *84*, 37–52. [[CrossRef](#)]
118. Zheng, E.H.; Xiong, J.J.; Luo, J.L. Second order sliding mode control for a quadrotor UAV. *ISA Trans.* **2014**, *53*, 1350–1356. [[CrossRef](#)]
119. Xiong, J.J.; Zheng, E.H. Position and attitude tracking control for a quadrotor UAV. *ISA Trans.* **2014**, *53*, 725–731. [[CrossRef](#)] [[PubMed](#)]
120. Jayakrishnan, H. Position and attitude control of a quadrotor UAV using super twisting sliding mode. *IFAC-PapersOnLine* **2016**, *49*, 284–289. [[CrossRef](#)]
121. Xu, B. Composite learning finite-time control with application to quadrotors. *IEEE Trans. Syst. Man. Cybern. Syst.* **2017**, *48*, 1806–1815. [[CrossRef](#)]
122. Jia, Z.; Yu, J.; Mei, Y.; Chen, Y.; Shen, Y.; Ai, X. Integral backstepping sliding mode control for quadrotor helicopter under external uncertain disturbances. *Aerosp. Sci. Technol.* **2017**, *68*, 299–307. [[CrossRef](#)]
123. Xiong, J.J.; Zhang, G.B. Global fast dynamic terminal sliding mode control for a quadrotor UAV. *ISA Trans.* **2017**, *66*, 233–240. [[CrossRef](#)] [[PubMed](#)]
124. Nekoukar, V.; Dehkordi, N.M. Robust path tracking of a quadrotor using adaptive fuzzy terminal sliding mode control. *Control Eng. Pract.* **2021**, *110*, 104763. [[CrossRef](#)]
125. Ríos, H.; Falcón, R.; González, O.A.; Dzul, A. Continuous sliding-mode control strategies for quadrotor robust tracking: Real-time application. *IEEE Trans. Ind. Electron.* **2019**, *66*, 1264–1272. [[CrossRef](#)]
126. Zhao, B.; Xian, B.; Zhang, Y.; Zhang, X. Nonlinear robust adaptive tracking control of a quadrotor UAV via immersion and invariance methodology. *IEEE Trans. Ind. Electron.* **2014**, *62*, 2891–2902. [[CrossRef](#)]
127. Cabecinhas, D.; Cunha, R.; Silvestre, C. A nonlinear quadrotor trajectory tracking controller with disturbance rejection. *Control Eng. Pract.* **2014**, *26*, 1–10. [[CrossRef](#)]
128. Ha, C.; Zuo, Z.; Choi, F.B.; Lee, D. Passivity-based adaptive backstepping control of quadrotor-type UAVs. *Robot. Auton. Syst.* **2014**, *62*, 1305–1315. [[CrossRef](#)]

129. Islam, S.; Liu, P.X.; El Saddik, A. Robust control of four-rotor unmanned aerial vehicle with disturbance uncertainty. *IEEE Trans. Ind. Electron.* **2015**, *62*, 1563–1571. [[CrossRef](#)]
130. Ma, D.; Xia, Y.; Li, T.; Chang, K. Active disturbance rejection and predictive control strategy for a quadrotor helicopter. *IET Control Theory Appl.* **2016**, *10*, 2213–2222. [[CrossRef](#)]
131. Liu, H.; Li, D.; Zuo, Z.; Zhong, Y. Robust three-loop trajectory tracking control for quadrotors with multiple uncertainties. *IEEE Trans. Ind. Electron.* **2016**, *63*, 2263–2274. [[CrossRef](#)]
132. Wang, C.; Song, B.; Huang, P.; Tang, C. Trajectory tracking control for quadrotor robot subject to payload variation and wind gust disturbance. *J. Intell. Robot. Syst.* **2016**, *83*, 315–333. [[CrossRef](#)]
133. Xiao, B.; Yin, S. A new disturbance attenuation control scheme for quadrotor unmanned aerial vehicles. *IEEE Trans. Ind. Inform.* **2017**, *13*, 2922–2932. [[CrossRef](#)]
134. Liu, H.; Zhao, W.; Zuo, Z.; Zhong, Y. Robust control for quadrotors with multiple time-varying uncertainties and delays. *IEEE Trans. Ind. Electron.* **2017**, *64*, 1303–1312. [[CrossRef](#)]
135. Zuo, Z.; Mallikarjunan, S. L1 Adaptive Backstepping for Robust Trajectory Tracking of UAVs. *IEEE Trans. Ind. Electron.* **2016**, *64*, 2944–2954. [[CrossRef](#)]
136. Li, C.; Zhang, Y.; Li, P. Full control of a quadrotor using parameter-scheduled backstepping method: Implementation and experimental tests. *Nonlinear Dyn.* **2017**, *89*, 1259–1278. [[CrossRef](#)]
137. Chen, M.; Xiong, S.; Wu, Q. Tracking flight control of quadrotor based on disturbance observer. *IEEE Trans. Syst. Man. Cybern. Syst.* **2019**, *51*, 1414–1423. [[CrossRef](#)]
138. Guo, K.; Jia, J.; Yu, X.; Guo, L.; Xie, L. Multiple observers based anti-disturbance control for a quadrotor UAV against payload and wind disturbances. *Control Eng. Pract.* **2020**, *102*, 104560. [[CrossRef](#)]
139. Bisheban, M.; Lee, T. Geometric adaptive control with neural networks for a quadrotor in wind fields. *IEEE Trans. Control. Syst. Technol.* **2020**, *29*, 1533–1548. [[CrossRef](#)]
140. Hua, H.; Fang, Y.; Zhang, X.; Lu, B. A novel robust observer-based nonlinear trajectory tracking control strategy for quadrotors. *IEEE Trans. Control Syst. Technol.* **2020**, *29*, 1952–1963. [[CrossRef](#)]
141. Cervantes-Rojas, J.S.; Muñoz, F.; Chairez, I.; González-Hernández, I.; Salazar, S. Adaptive tracking control of an unmanned aerial system based on a dynamic neural-fuzzy disturbance estimator. *ISA Trans.* **2020**, *101*, 309–326. [[CrossRef](#)]
142. Chen, Z.; Nian, X.; Xu, P.; Wu, H. Robust Adaptive Tracking Control of a Quadrotor Helicopter with Uncertainties. In Proceedings of the 2021 40th Chinese Control Conference (CCC), Shanghai, China, 26–28 June 2021; p. 7748.
143. Liu, P.; Ye, R.; Shi, K.; Yan, B. Full backstepping control in dynamic systems with air disturbances optimal estimation of a quadrotor. *IEEE Access* **2021**, *9*, 34206–34220. [[CrossRef](#)]
144. Chen, L.; Liu, Z.; Dang, Q.; Zhao, W.; Wang, G. Robust trajectory tracking control for a quadrotor using recursive sliding mode control and nonlinear extended state observer. *Aerosp. Sci. Technol.* **2022**, *128*, 107749. [[CrossRef](#)]
145. Liang, W.; Chen, Z.; Yao, B. Geometric adaptive robust hierarchical control for quadrotors with aerodynamic damping and complete inertia compensation. *IEEE Trans. Ind. Electron.* **2022**, *69*, 13213–13224. [[CrossRef](#)]
146. Li, S.; Sun, Z. A generalized proportional integral observer-based robust tracking design approach for quadrotor unmanned aerial vehicle. *Int. J. Adv. Robot. Syst.* **2022**, *19*, 17298806221117052. [[CrossRef](#)]
147. Zhang, X.; Zhuang, Y.; Zhang, X.; Fang, Y. A Novel Asymptotic Robust Tracking Control Strategy for Rotorcraft UAVs. *IEEE Trans. Autom. Sci. Eng.* **2023**, *20*, 2338–2349. [[CrossRef](#)]
148. Yogi, S.C.; Kamath, A.K.; Singh, P.; Behera, L. Trajectory Tracking Control of a Quadrotor UAV using an Auto-tuning Robust Sliding Mode Controller. In Proceedings of the 2022 International Conference on Unmanned Aircraft Systems (ICUAS), Dubrovnik, Croatia, 21–24 June 2022; pp. 345–353.
149. Lopez-Sanchez, I.; Moyrón, J.; Moreno-Valenzuela, J. Adaptive neural network-based trajectory tracking outer loop control for a quadrotor. *Aerosp. Sci. Technol.* **2022**, *129*, 107847. [[CrossRef](#)]
150. Kong, L.; Reis, J.; He, W.; Silvestre, C. Experimental Validation of a Robust Prescribed Performance Nonlinear Controller for an Unmanned Aerial Vehicle With Unknown Mass. *IEEE/ASME Trans. Mechatron.* **2023**, early access. [[CrossRef](#)]
151. Labbadi, M.; Cherkaoui, M. Robust adaptive backstepping fast terminal sliding mode controller for uncertain quadrotor UAV. *Aerosp. Sci. Technol.* **2019**, *93*, 105306. [[CrossRef](#)]
152. Shao, X.; Liu, J.; Cao, H.; Shen, C.; Wang, H. Robust dynamic surface trajectory tracking control for a quadrotor UAV via extended state observer. *Int. J. Robust Nonlinear Control* **2018**, *28*, 2700–2719. [[CrossRef](#)]
153. Wang, R.; Liu, J. Trajectory tracking control of a 6-DOF quadrotor UAV with input saturation via backstepping. *J. Frankl. Inst.* **2018**, *355*, 3288–3309. [[CrossRef](#)]
154. Zuo, Z.; Wang, C. Adaptive trajectory tracking control of output constrained multi-rotors systems. *IET Control Theory Appl.* **2014**, *8*, 1163–1174. [[CrossRef](#)]
155. Song, Y.; He, L.; Zhang, D.; Qian, J.; Fu, J. Neuroadaptive fault-tolerant control of quadrotor UAVs: A more affordable solution. *IEEE Trans. Neural Netw. Learn. Syst.* **2018**, *30*, 1975–1983. [[CrossRef](#)] [[PubMed](#)]
156. Mofid, O.; Mobayen, S. Adaptive sliding mode control for finite-time stability of quad-rotor UAVs with parametric uncertainties. *ISA Trans.* **2018**, *72*, 1–14. [[CrossRef](#)] [[PubMed](#)]

157. Baca, T.; Petrlik, M.; Vrba, M.; Spurny, V.; Penicka, R.; Hert, D.; Saska, M. The MRS UAV system: Pushing the frontiers of reproducible research, real-world deployment, and education with autonomous unmanned aerial vehicles. *J. Intell. Robot. Syst.* **2021**, *102*, 26. [[CrossRef](#)]
158. Baca, T.; Hert, D.; Loianno, G.; Saska, M.; Kumar, V. Model predictive trajectory tracking and collision avoidance for reliable outdoor deployment of unmanned aerial vehicles. In Proceedings of the 2018 IEEE/RSJ International Conference on Intelligent Robots and Systems (IROS), Madrid, Spain, 1–5 October 2018; pp. 6753–6760.
159. Yang, J.; Cai, Z.; Zhao, J.; Wang, Z.; Ding, Y.; Wang, Y. INDI-based aggressive quadrotor flight control with position and attitude constraints. *Robot. Auton. Syst.* **2023**, *159*, 104292. [[CrossRef](#)]
160. El Houm, Y.; Abbou, A.; Labbadi, M.; Cherkaoui, M. Optimal new sliding mode controller combined with modified supertwisting algorithm for a perturbed quadrotor UAV. *Int. J. Aerosp. Eng.* **2020**, *2020*, 1–10. [[CrossRef](#)]

**Disclaimer/Publisher’s Note:** The statements, opinions and data contained in all publications are solely those of the individual author(s) and contributor(s) and not of MDPI and/or the editor(s). MDPI and/or the editor(s) disclaim responsibility for any injury to people or property resulting from any ideas, methods, instructions or products referred to in the content.